Soil Dynamics and Earthquake Engineering 144 (2021) 106642

Contents lists available at ScienceDirect

Soil Dynamics and Earthquake Engineering

journal homepage: http://www.elsevier.com/locate/soildyn

Variable seismic motions of P-wave scattering by a layered V-shaped canyon of the second stratification type

Guohuan Liu [a,b,*], Guangrui Feng [a,b]

[a] State Key Laboratory of Hydraulic Engineering Simulation and Safety, Tianjin University, Tianjin, 300072, China
[b] School of Civil Engineering, Tianjin University, Tianjin, 300072, China

ARTICLE INFO

Keywords:
Variable earthquake motions
V-shaped canyon
Wave scattering

ABSTRACT

Seismic waves scattering especially waves SH by different topographies has been widely studied in the field of earthquake engineering. However, most of these studies mainly focus on the topographies with the ideal assumption (elastic, isotropic and homogeneous) of uniform medium or the first stratification type of canyon (canyon that is not crossing by layer-interfaces). Compared with SH wave scattering, there exists a challenge to derive the theoretical solution for the scattering of P or SV wave especially by relative complicated canyon with non-uniform medium, which is defined as the second stratification type or type II here. The paper focuses on the study on the two-dimensional scattering of plane P waves by a symmetrical V-shaped canyon embedded in a two-layered elastic half-plane of type II. The challenge is to deal with three issues simultaneously, namely satisfaction of boundary conditions in the vertical direction, more complex reflections and more coordinate system transformations. Here more cylindrical coordinate systems and the skew coordinate transformation formulas need to be defined and used so as to satisfy the boundary conditions along the canyon surface, in which coordinate transformation and its solution process become more complex. The derived solution of symmetrical V-shaped canyon is rigorous theoretically and reliable, and further demonstrate that it is affected directly by the second layered type of symmetrical V-shaped canyon. Moreover, the effects of the layer medium, the incident frequencies and incident angles on the ground motion also are investigated by the double-layer considering nonhomogeneous cases. This study shows that inhomogeneous-material, frequencies of incident waves and the existence of the canyon result in conspicuous even non-ignorable effect on variability of surface ground motions.

1. Introduction

It has been observed that the seismic spatial variability influenced significantly the response of the large-span structures (e.g. crossing canyon bridges dams in valley, subways, tunnels through mountain) [1–6]. These structures are usually constructed on the sites of topographic irregularities. The site effect of local inhomogeneity and irregularity on variable seismic motions induced scattering of seismic waves is one of the most topical issues in seismology and aseismic engineering. Over the past decades, the scattering and diffraction of seismic waves by irregular topography features have been intensively studies in the community of earthquake engineering, and can be theoretically investigated by numerical and (or) analytical method. Generally, numerical methods such as finite difference methods [7], finite element methods [8]and boundary element methods [9–12] play a vital role in solving practical complicated problems [13–17] and dealing with complex boundary conditions [18–21]. However, there exists certain limitations to tackle the valid solution of scattering induced seismic waves in the broad frequency band with numerical method, and it also fails to reveal the mechanism of seismic waves scattering in physics. Meanwhile, the theoretical solutions can be used to verify accuracy of the analysis results by numerical methods as to the topographies presumed regular geometries. Therefore, the development of theoretical solutions to the regular canyon topographies is requisite from perspectives of both theory and practice.

To derive the theoretical solutions of SH wave scattering by the regular canyon topographies (the semi-circular canyon and the semi-elliptic canyon), the method for expressing the wave functions was introduced firstly by Trifunac [22,23]. Based on the work of Trifunac, many scholars and researchers have made many achievements in the field of study, and presented some theoretical solutions of plane SH waves scattering by canyon surface for different cases as well, such as a

* Corresponding author. School of Civil Engineering, Tianjin University, Tianjin, 300072, China
E-mail address: liugh@tju.edu.cn (G. Liu).

https://doi.org/10.1016/j.soildyn.2021.106642
Received 25 August 2020; Received in revised form 22 November 2020; Accepted 31 January 2021
0267-7261/© 2021 Elsevier Ltd. All rights reserved.

symmetrical shallow V-shaped canyon [24], a symmetrical deep V-shaped canyon [25], the symmetrical V-shaped canyon [26], the non-symmetrical V-shaped canyon [27], the truncated semicircular canyon [28], the U-shaped canyon [29], and the cylindrical canyon [30–35]. Unlike the scattering process of SH wave, the physical process of scattering of P or SV waves by the irregular canyon topographies are more complex due to the existence of more reflected and transmitted scattering waves (e.g. P and SV). The effect of relatively simple canyon topographies (circular-arc layered alluvial valley, and multiple circular-arc etc) on vertical plane waves scattering was studied by the many scholars [36–38]. A proper form of stress-free wave function was redefined by Lee and Liu to solve analytically the two-dimensional scattering problems of plane P and SV waves around a semi-circular canyon in an elastic half-plane [39]. In all, the research significance has been realized by more scholars and many significant progresses have been made over the past decades.

However, the past study is mainly focused on the seismic waves scattering especially SH waves, and usually assumed the assumption of uniform medium or the first stratification type which is defined as the first stratification type or type I here. Compared with SH waves scattering, there exists a challenge to derive the theoretical solution for P or SV wave scattering especially by relative complicated canyon with non-uniform medium, which is defined as the second stratification type or type II here. This paper focuses on study on the effect of the symmetrical V-shaped canyon embedded in a two-layered elastic half-pane of type II on the scattering of plane P waves. Compared with the symmetrical V-shaped canyon embedded in a two-layered elastic half-plane of type I, the challenge is to deal with three issues simultaneously. Firstly, the boundary conditions along the canyon surface (especially layer-interface) need to be satisfied. Secondly, along the surface layer-interface crossing canyon, the transmitted waves and reflected waves are produced than the unstratified site. Finally, more complicated coordinate transformations (e.g. skew coordinate transformation) need to be applied because of more scattering waves. Moreover, along the canyon surface and layer-interface boundaries in the canyon of type II (the specific difference is discussed and given in section 2.1), there are more difficulties in dealing with the P and SV waves scattering problems. In order to use the wave function expansion method, P or SV waves must be expressed in the form of potential function. Furthermore, to satisfy the zero-stress boundary conditions, the potential functions of both P and SV waves need satisfy pairwise orthogonal at the half-plane. However, the potential functions of the scattered vertical plane waves by the canyon surface cannot satisfy pairwise orthogonal at the half-plane as they are defined in whatever O_1, O_2 or O coordinates systems (see

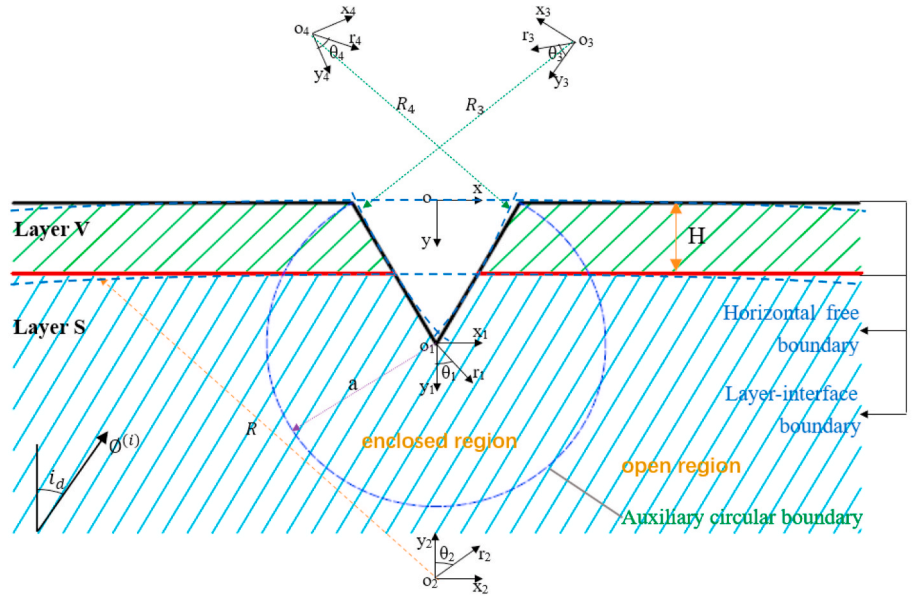

(a) Layer-interface crossing canyon (the second stratification type)

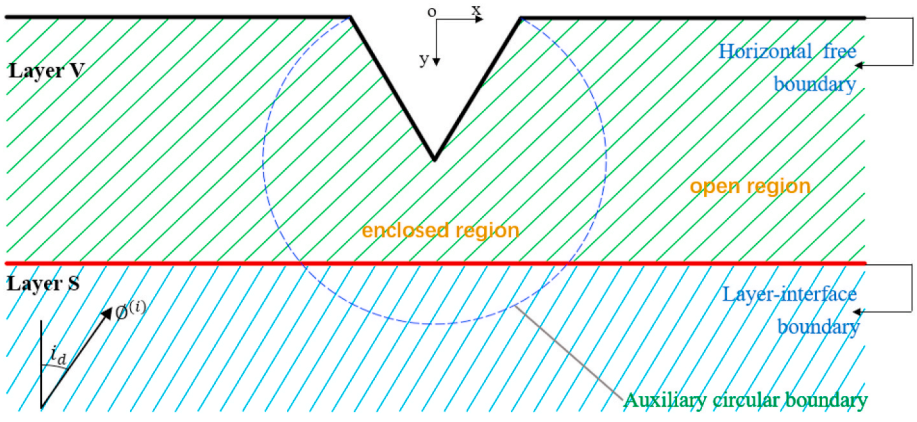

(b) Layer-interface not crossing canyon (the first stratification type)

Fig. 1. Canyon topography model.

Fig. 1). So, the result will lead to that the zero-stress boundary conditions along the V-shaped canyon surface cannot be satisfied. Based on above discussion, additional O_3 and O_4 coordinate systems need to be defined to satisfy the zero-stress boundary conditions along the symmetrical V-shaped canyon surface, respectively. To illustrate the research significance more clearly, the essential differences between the type II and I are given specifically in section 2.1. Therefore, in order to satisfy zero-stress boundary conditions along canyon surface, more coordinate systems need to be established and which results more complicated solution procedure. Based on the solution derived, the effects of the layer medium, the incident frequencies and incident angles on the ground motion are further investigated. Results show that the ideal assumption of uniform medium should be adopted carefully.

2. Model and theoretical formulation

The model of the canyon with two layers (Layer-V and Layer-S) subjected by the harmonic incident P waves is shown in Fig. 1(a). The medium of both layers is assumed to be elastic, isotropic and homogeneous. The material properties of each layer are determined on the Lame coefficients λ_v, λ_s, μ_v, μ_s and mass density ρ_v, ρ_s, where the subscripts v, s denote Layer-V and Layer-S, respectively. The wave velocities of the P and SV waves in each layer are denoted α_v, β_v, and α_s, β_s respectively. A plane global Cartesian co-ordinate system *xoy* and four proper local co-ordinate systems x_iOy_i are located at proper corresponding position (see Fig. 1(a)) to facilitating solution later, where $i = 1,2,3,4$ and the angle θ_i is measured from the vertical y_i-axis counterclockwise towards the x_i-axis with a positive direction to the right. An auxiliary circular arc boundary is established with the center O_1 and the radius a to solve the unknown coefficient which will divide whole area to be solved into two regions including open region and enclosed region. Detailed descriptions of various reflected waves and scattered waves are given in section 2.2 and section 2.3 later in this paper.

The harmonic P wave propagates with circular frequency ω and incident angle i_d, its potential function is denoted in global rectangular coordinate system by

$$\Phi^{(i)}(x,y) = \exp[ik_{s\alpha}(x\sin i_d - y\cos i_d)] \tag{1}$$

in which i is the imaginary unit, $k_{s\alpha} = \omega/\alpha_s$ is the wave number of the longitudinal P wave in the half-plane, and the time factor $\exp(-i\omega t)$ is omitted.

2.1. Essential difference between type I and II

The difference between the two stratification types of V-shaped canyon excited by incident P or SV waves is discussed and given from perspective of physics and mathematics.

(1) As for the aspect of physical phenomenon

Compared with the type I shown in Fig. 1(b), more scattering waves are produced on the V-shaped canyon boundaries due to the existence of inhomogeneous-material that coming with the layer-interface crossing the canyon boundaries, which directly lead to more complex solution process.

(2) From perspective of mathematical expression

More scattering waves will lead to the increasement of the number of unknown coefficients (equation coefficients), which will logically result in more complex solutions. Specifically, on the one hand, it is necessary to simultaneously meet the two levels of zero stress conditions instead of single level at the canyon boundaries, which leads to more complex computing processes (more equations need to be solved) beyond all doubt. On the other hand, more coordinate transformations and equations need to be done and solved to satisfy the displacement continuous conditions on the layer-interface. Moreover, the potential risk of matrix singularity will be greatly increased due to the inversion of higher dimensional matrix coming from more coordinate transformations and equation coefficients to solve, which increases the probability of solution difficulty in theory.

In all, the complexity and difficulty of solving the theoretical solution for the second stratification type is increased respectively. The solutions of scattering wave field are showed in section 2.3.

2.2. Free wave field

The reflected and the transmitted P and SV waves are generated at the free-surface and at the layered interface of the half-plane if there is no canyon case (see Fig. 2). The wave potential functions of the P and SV waves can be denoted in terms of the global Cartesian co-ordinate system as follows

$$\Phi^{(r)}(x,y) = ks1\exp[ik_{s\alpha}(x\sin i_d + (y-d)\cos i_d)] \tag{2}$$

$$\Psi^{(r)}(x,y) = ks2\exp[ik_{s\beta}(x\sin i_s + (y-d)\cos i_s)] \tag{3}$$

$$\Phi^{(t)}(x,y) = t_1\exp[ik_{v\alpha}(x\sin t_d - (y-d)\cos t_d)] \tag{4}$$

$$\Psi^{(t)}(x,y) = t_2\exp[ik_{v\beta}(x\sin t_s - (y-d)\cos t_s)] \tag{5}$$

$$\Phi^{(r)}_{vp}(x,y) = k_{p1v}t_1\exp[ik_{v\alpha}(x\sin t_d + y\cos t_d)] \tag{6}$$

$$\Psi^{(r)}_{vp}(x,y) = k_{p2v}t_1\exp\left[ik_{v\beta}\left(x\sin i_{vp} + y\cos i_{vp}\right)\right] \tag{7}$$

$$\Phi^{(r)}_{vs}(x,y) = k_{s1v}t_2\exp[ik_{v\alpha}(x\sin i_{vs} + y\cos i_{vs})] \tag{8}$$

$$\Psi^{(r)}_{vs}(x,y) = k_{s2v}t_2\exp[ik_{v\beta}(x\sin t_s + y\cos t_s)] \tag{9}$$

where $k_{s\beta} = \omega/\beta_s$ is the wave number of the shear SV waves in the half-plane, $k_{v\alpha} = \omega/\alpha_v$ and $k_{v\beta} = \omega/\beta_v$ are the numbers of the P wave and the SV waves in the layer-V, respectively. k_{s1}, k_{s2}, t_1, t_2, k_{p1v}, k_{p2v}, k_{s1v}, k_{s2v} are separately reflection and transmittance coefficients, which are showed in the appendix-A1.

Different reflected P and SV waves are generated as a result of variation in ration of incident angle i_d to critical angle $\theta_{cr} = \sin^{-1}(\alpha_s/\beta_s)$ in the case of the P waves incident topography. In order to simplify the analysis, this paper only consider $i_d < \theta_{cr}$.

For convenience, Eqs. (1)–(9) are transformed into coordinate system r_1-θ_1:

$$\Phi^{(i)}(r_1,\theta_1) = \exp[-ik_{s\alpha}r_1\cos(\theta_1 + i_d) - id_2k_{s\alpha}\cos i_d] \tag{10}$$

$$\Phi^{(r)}(r_1,\theta_1) = k_{s1}\exp[ik_{s\alpha}r_1\cos(\theta_1 - i_d) + id_2k_{s\alpha}\cos i_d] \tag{11}$$

$$\Psi^{(r)}(r_1,\theta_1) = k_{s2}\exp[ik_{s\beta}r_1\cos(\theta_1 - i_s) + id_2k_{s\beta}\cos i_s] \tag{12}$$

$$\Phi^{(t)}(r_1,\theta_1) = t_1\exp[-ik_{v\alpha}r_1\cos(\theta_1 + t_d) - id_2k_{v\alpha}\cos t_d] \tag{13}$$

$$\Phi^{(t)}(r_1,\theta_1) = t_2\exp[-ik_{v\beta}r_1\cos(\theta_1 + t_s) - id_2k_{v\beta}\cos t_s] \tag{14}$$

$$\Phi^{(r)}_{vp}(r_1,\theta_1) = k_{p1v}t_1\exp[ik_{v\alpha}r_1\cos(\theta_1 - t_d) + id_2k_{v\alpha}\cos t_d] \tag{15}$$

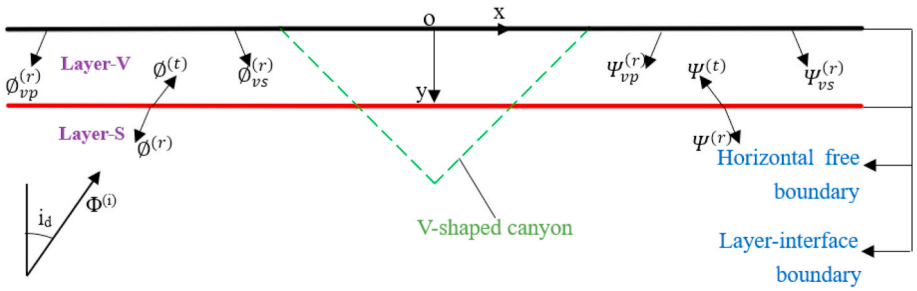

Fig. 2. The free wave field diagram.

$$\Psi_{vp}^{(r)}(r_1,\theta_1)=k_{p2v}t_1\exp\left[ik_{v\beta}r_1\cos\left(\theta_1-i_{vp}\right)+id_2k_{v\beta}\cos i_{vp}\right] \tag{16}$$

$$\Phi_{vp}^{(r)}(r_1,\theta_1)=k_{p1v}t_1\exp[ik_{v\alpha}r_1\cos(\theta_1-t_d)+id_2k_{v\alpha}\cos t_d] \tag{17}$$

$$\Psi_{vs}^{(r)}(r_1,\theta_1)=k_{s2v}t_2\exp[ik_{v\beta}r_1\cos(\theta_1-t_s)+id_2k_{v\beta}\cos t_s] \tag{18}$$

Combining Eqs. (10)–(11), (13)–(15) and (14)–(16) and then expanding them into Fourier-Bessel series:

$$\exp(\pm ikr\cos\theta)=\sum_{n=0}^{\infty}\varepsilon_n(\pm i)^nJ_n(kr)\cos n\theta \tag{19}$$

and

$$\Phi_{vs}^{(i+r)}(r_1,\theta_1)=\sum_{m=0}^{\infty}J_m(k_{s\alpha}r_1)\left(A_{0,m}\cos m\theta_1+B_{0,m}\sin m\theta_1\right) \tag{20}$$

$$\Psi_{vs}^{(r)}(r_1,\theta_1)=\sum_{m=0}^{\infty}J_m(k_{s\beta}r_1)\left(C_{0,m}\sin m\theta_1+D_{0,m}\cos m\theta\right)_1 \tag{21}$$

$$\Phi^{(i+r)}(r_1,\theta_1)=\sum_{m=0}^{\infty}J_m(k_{v\alpha}r_1)\left(A_{1,m}\cos m\theta_1+B_{1,m}\sin m\theta_1\right) \tag{22}$$

$$\psi^{(i+r)}(r_1,\theta_1)=\sum_{m=0}^{\infty}J_m(k_{v\beta}r_1)\left(C_{1,m}\sin m\theta_1+D_{1,m}\cos m\theta_1\right) \tag{23}$$

Where $A_{0,m}$-$D_{1,m}$ are showed in the appendix-A1.

2.3. Scattering wave field

In this study, the horizontal ground surface, the horizontal layer-interface and canyon boundary are approximated by the almost-flat circular boundaries with large radius R (R»a). The research shows that the error can be controlled within the effective range while the radius R is large enough such as R = 100a [36].

The scattered P and SV waves generated by V-shaped canyon, the horizontal ground surface and the layer-interface boundary in Layer-S can be expressed as follows, respectively. In the open region, there are scattered P wave $\Phi_{s1}(r_2, \theta_2)$ and SV wave $\Psi_{s1}(r_2, \theta_2)$ generated by the circular boundary of large radius approximating layer-interface boundary, and scattered P wave $\Phi_{s0}(r_1, \theta_1)$, $\Phi_{s2}(r_1, \theta_1)$ and SV waves $\Psi_{s0}(r_1, \theta_1)$, $\Psi_{s2}(r_1, \theta_1)$, generated by the canyon surface boundary in the Layer-S; scattered P waves $\Phi_{v1}(r_2, \theta_2)$, $\Phi_{v0}(r_1, \theta_1)$, $\Phi_{v2}(r_1, \theta_1)$, $\Phi_{v5}(r_2, \theta_2)$ and SV waves $\Psi_{v1}(r_2, \theta_2)$, $\Psi_{v0}(r_1, \theta_1)$, $\Psi_{v2}(r_1, \theta_1)$, $\Psi_{v5}(r_2, \theta_2)$ generated by circular boundary of large radius approximating the ground surface

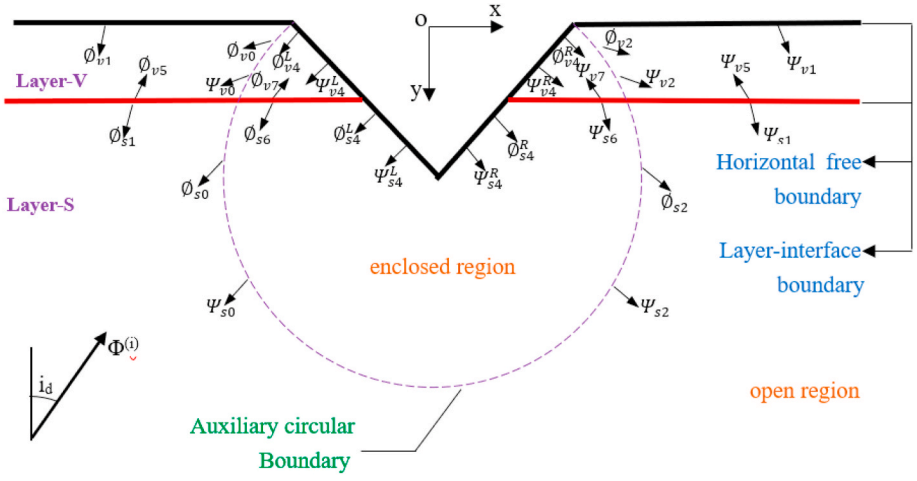

Fig. 3. The scattering wave field diagram.

boundary in the Layer-V. In the enclosed region, there are scattered P waves $\Phi_{s4L}(r_3, \theta_3)$, $\Phi_{s4R}(r_4, \theta_4)$ and SV waves $\Psi_{s4L}(r_3, \theta_3)$, $\Psi_{s4R}(r_4, \theta_4)$ generated by the canyon surface boundary, and scattered P wave $\Phi_{s6}(r_2, \theta_2)$ and SV wave $\Psi_{s6}(r_2, \theta_2)$ generated by the circular boundary of large radius approximating layer-interface boundary in the Layer-S; scattered P waves $\Phi_{v4L}(r_3, \theta_3)$, $\Phi_{v4R}(r_4, \theta_4)$ and SV waves$\Psi_{v4L}(r_3, \theta_3)$, $\Psi_{v4R}(r_4, \theta_4)$ generated by the canyon surface boundary, and scattered wave $\Phi_{v7}(r_2, \theta_2)$ and scattered SV wave $\Psi_{s0}(r_1, \theta_1)$ generated by the circular boundary of large radius approximating layer-interface boundary in the Layer-V (see Fig. 3).

Therefore, the wave potential functions in each region can be written as, these waves can be expressed as Fourier-Bessel series (see appendix-C).

the auxiliary arc boundary:

$$\begin{cases} \tau_{r\theta}^{v(o)} = \tau_{r\theta}^{v(c)}, (r_1 = a, -\delta_1 \le \theta_1 \le -\partial_1, \partial_1 \le \theta_1 \le \delta_1) \\ \tau_{r\theta}^{s(o)} = \tau_{r\theta}^{s(c)}, (r_1 = a, -\partial_1 \le \theta_1 \le \partial_1) \\ \tau_{rr}^{v(o)} = \tau_{rr}^{v(c)}, (r_1 = a, -\delta_1 \le \theta_1 \le -\partial_1, \partial_1 \le \theta_1 \le \delta_1) \\ \tau_{rr}^{s(o)} = \tau_{rr}^{s(c)}, (r_1 = a, -\partial_1 \le \theta_1 \le \partial_1) \\ u_r^{v(o)} = u_r^{v(c)}, (r_1 = a, -\delta_1 \le \theta_1 \le -\partial_1, \partial_1 \le \theta_1 \le \delta_1) \\ u_r^{s(o)} = u_r^{s(c)}, (r_1 = a, -\partial_1 \le \theta_1 \le \partial_1) \\ u_\theta^{v(o)} = u_\theta^{v(c)}, (r_1 = a, -\delta_1 \le \theta_1 \le -\partial_1, \partial_1 \le \theta_1 \le \delta_1) \\ u_\theta^{s(o)} = u_\theta^{s(c)}, (r_1 = a, -\partial_1 \le \theta_1 \le \partial_1) \end{cases} \tag{26}$$

- open region
  - Layer-S: $\Phi_{s1}(r_2, \theta_2)$, $\Psi_{s1}(r_2, \theta_2)$, $\Phi_{s0}(r_1, \theta_1)$, $\Psi_{s0}(r_1, \theta_1)$, $\Phi_{s2}(r_1, \theta_1)$, $\Psi_{s2}(r_1, \theta_1)$
  - Layer-V
    - L: $\Phi_{v1}(r_2, \theta_2)$, $\Psi_{v1}(r_2, \theta_2)$, $\Phi_{v0}(r_1, \theta_1)$, $\Psi_{v0}(r_1, \theta_1)$, $\Phi_{v5}(r_1, \theta_1)$, $\Psi_{v5}(r_1, \theta_1)$
    - R: $\Phi_{v1}(r_2, \theta_2)$, $\Psi_{v1}(r_2, \theta_2)$, $\Phi_{v2}(r_1, \theta_1)$, $\Psi_{v2}(r_1, \theta_1)$, $\Phi_{v5}(r_2, \theta_2)$, $\Psi_{v5}(r_2, \theta_2)$
- enclosed region
  - Layer-S: $\Phi_{s4L}(r_3, \theta_3)$, $\Psi_{s4L}(r_3, \theta_3)$, $\Phi_{s4R}(r_4, \theta_4)$, $\Psi_{s4R}(r_4, \theta_4)$, $\Phi_{s6}(r_2, \theta_2)$, $\Psi_{s6}(r_2, \theta_2)$
  - Layer-V
    - L: $\Phi_{v4L}(r_3, \theta_3)$, $\Psi_{v4L}(r_3, \theta_3)$, $\Phi_{v7}(r_2, \theta_2)$, $\Psi_{v7}(r_2, \theta_2)$
    - R: $\Phi_{v4R}(r_4, \theta_4)$, $\Psi_{v4R}(r_4, \theta_4)$, $\Phi_{v7}(r_2, \theta_2)$, $\Psi_{v7}(r_2, \theta_2)$

2.4. Satisfaction of boundary conditions

The waves must satisfy the traction-free boundary condition at the ground surface and the canyon surface. Meanwhile, the waves must also satisfy both the continuity conditions of the displacement and stress-field at the layer-interface and the auxiliary arc circular, respectively. The boundary conditions of each region can be expressed as follow

Open region:

$$\begin{cases} \tau_{rr}^{v(o)} = \tau_{r\theta}^{v(o)} = 0, (r_2 = R + h) \\ \tau_{rr}^{v(o)} = \tau_{rr}^{s(o)}, \tau_{r\theta}^{v(o)} = \tau_{r\theta}^{s(o)}, (r_2 = R) \\ u_r^{v(o)} = u_r^{s(o)}, u_\theta^{v(o)} = u_\theta^{s(o)}, (r_2 = R) \end{cases} \tag{24}$$

Enclosed region:

$$\begin{cases} \tau_{rr}^{v(c)} = \tau_{r\theta}^{v(c)} = 0, (r_3 = R_3, -\delta_3 \le \theta_3 \le 0) \\ \tau_{rr}^{s(c)} = \tau_{r\theta}^{s(c)} = 0, (r_3 = R_3, 0 \le \theta_3 \le \delta_3) \\ \tau_{rr}^{s(c)} = \tau_{r\theta}^{s(c)} = 0, (r_3 = R_3, 0 \le \theta_3 \le \delta_3) \\ \tau_{rr}^{s(c)} = \tau_{r\theta}^{s(c)} = 0, (r_3 = R_3, 0 \le \theta_3 \le \delta_3) \end{cases} \tag{25}$$

The displacements and stresses of a plane strain problem for incident P wave can be expressed as [27].

(1) Open region:

Applying the boundary condition $\tau_{rr}^{v(c)} = \tau_{r\theta}^{v(c)} = 0, (r_3 = R + H)$, we have

$$\begin{Bmatrix} A_{v1,n}^{(2)} + A_{v0,n}^{(2)} \\ C_{v1,n}^{(2)} + C_{v0,n}^{(2)} \end{Bmatrix} = \begin{bmatrix} XA11_n & XA12_n \\ XC11_n & XC12_n \end{bmatrix} \begin{Bmatrix} A_{v5,n}^{(2)} \\ C_{v5,n}^{(2)} \end{Bmatrix} = \begin{Bmatrix} A_{v1,n}^{(2)} + A_{v2,n}^{(2)} \\ C_{v1,n}^{(2)} + C_{v2,n}^{(2)} \end{Bmatrix} \tag{27a}$$

$$\begin{Bmatrix} B_{v1,n}^{(2)} + B_{v0,n}^{(2)} \\ D_{v1,n}^{(2)} + D_{v0,n}^{(2)} \end{Bmatrix} = \begin{bmatrix} XB11_n & XB12_n \\ XD11_n & XD12_n \end{bmatrix} \begin{Bmatrix} B_{v5,n}^{(2)} \\ D_{v5,n}^{(2)} \end{Bmatrix} = \begin{Bmatrix} B_{v1,n}^{(2)} + B_{v2,n}^{(2)} \\ D_{v1,n}^{(2)} + D_{v2,n}^{(2)} \end{Bmatrix} \tag{27b}$$

Where

$$\begin{cases} XA11_n = \left[E_{22}^{v_o^{(1)}}(n, R+h)E_{11}^{v_o^{(3)}}(n, R+h) - E_{12}^{v_o^{(1)}+}(n, R+h)E_{21}^{v_o^{(3)}-}(n, R+h)\right] / (-\mathrm{Zn} \\ XA12_n = \left[E_{22}^{v_o^{(1)}}(n, R+h)E_{11}^{v_o^{(3)}}(n, R+h) - E_{12}^{v_o^{(1)}+}(n, R+h)E_{22}^{v_o^{(3)}-}(n, R+h)\right] / (-\mathrm{Zn} \\ XC11_n = \left[-E_{21}^{v_o^{(1)}-}(n, R+h)E_{11}^{v_o^{(3)}}(n, R+h) - E_{12}^{v_o^{(1)}+}(n, R+h)E_{21}^{v_o^{(3)}-}(n, R+h)\right] / (-\mathrm{Zn} \\ XC12_n = \left[-E_{21}^{v_o^{(1)-}}(n, R+h)E_{11}^{v_o^{(3)}}(n, R+h) - E_{12}^{v_o^{(1)}+}(n, R+h)E_{22}^{v_o^{(3)}-}(n, R+h)\right] / (-\mathrm{Zn} \\ Z = E_{11}^{v_o^{(1)}}(n, R+h)E_{11}^{v_o^{(3)}}(n, R+h) - E_{12}^{v_o^{(1)}+}(n, R+h)E_{21}^{v_o^{(3)}-}(n, R+h) \end{cases} \tag{28a}$$

$$\begin{cases} XB11_n = \left[E_{22}^{v_o^{(1)}}(n,R+h)E_{11}^{v_o^{(3)}}(n,R+h) - E_{12}^{v_o^{(1)}+}(n,R+h)E_{21}^{v_o^{(3)}-}(n,R+h)\right]\Big/(-Wn \\ XB12_n = \left[E_{22}^{v_o^{(1)}}(n,R+h)E_{11}^{v_o^{(3)}}(n,R+h) - E_{12}^{v_o^{(1)}+}(n,R+h)E_{22}^{v_o^{(3)}-}(n,R+h)\right]\Big/(-Wn \\ XD11_n = \left[-E_{21}^{v_o^{(1)}+}(n,R+h)E_{11}^{v_o^{(3)}}(n,R+h) - E_{12}^{v_o^{(1)}+}(n,R+h)E_{21}^{v_o^{(3)}-}(n,R+h)\right]\Big/(-Wn \\ XD12_n = \left[-E_{21}^{v_o^{(1)}+}(n,R+h)E_{11}^{v_o^{(3)}}(n,R+h) - E_{12}^{v_o^{(1)}+}(n,R+h)E_{22}^{v_o^{(3)}-}(n,R+h)\right]\Big/(-Wn \\ W = E_{11}^{v_o^{(1)}}(n,R+h)E_{11}^{v_o^{(3)}}(n,R+h) - E_{12}^{v_o^{(1)}+}(n,R+h)E_{21}^{v_o^{(3)}-}(n,R+h) \end{cases} \tag{28b}$$

Where $E_{ij}^{v_o^{(k)}}(n,r)I_{ij}^{v_o^{(K)}}(n,r)$ are showed in Appendix-D.

Applying the boundary conditions $u_r^{v(o)} = u_r^{s(o)}, u_\theta^{v(o)} = u_\theta^{s(o)}, (r_2 = R)$, we have:

$$\begin{Bmatrix} A_{v1,n}^{(2)} + A_{v2,n}^{(2)} + A_{1,n} \\ C_{v1,n}^{(2)} + C_{v0,n}^{(2)} + C_{1,n} \end{Bmatrix} = \begin{bmatrix} WA13_n & WC13_n \\ WA23_n & WC23_n \end{bmatrix} \begin{Bmatrix} A_{v5,n}^{(2)} \\ C_{v5,n}^{(2)} \end{Bmatrix} + \begin{bmatrix} VAA1_n & VAC1_n \\ VAA2_n & VAC2_n \end{bmatrix} \begin{Bmatrix} A_{s1,n}^{(2)} + A_{s2,n}^{(2)} + A_{s0,n}^{(2)} + A_{0,n} \\ C_{s1,n}^{(2)} + C_{s2,n}^{(2)} + C_{s0,n}^{(2)} + C_{0,n} \end{Bmatrix} \tag{29a}$$

$$\begin{Bmatrix} B_{v1,n}^{(2)} + B_{v2,n}^{(2)} + B_{1,n} \\ D_{v1,n}^{(2)} + D_{v0,n}^{(2)} + D_{1,n} \end{Bmatrix} = \begin{bmatrix} WB13_n & WD13_n \\ WB23_n & WD23_n \end{bmatrix} \begin{Bmatrix} B_{v5,n}^{(2)} \\ D_{v5,n}^{(2)} \end{Bmatrix} + \begin{bmatrix} VBB1_n & VBD1_n \\ VBB2_n & VBD2_n \end{bmatrix} \begin{Bmatrix} B_{s1,n}^{(2)} + B_{s2,n}^{(2)} + B_{s0,n}^{(2)} + B_{0,n} \\ D_{s1,n}^{(2)} + D_{s2,n}^{(2)} + D_{s0,n}^{(2)} + D_{0,n} \end{Bmatrix} \tag{29b}$$

Where unknown coefficients $WA13_n$, $VAA1_n$ can be easily determined by referring to Eq (28).

Applying the boundary conditions $\tau_{rr}^{v(o)} = \tau_{rr}^{s(o)}, \tau_{r\theta}^{v(o)} = \tau_{r\theta}^{s(o)}, (r_2 = R)$, the following equation is established:

$$\begin{Bmatrix} A_{v1,n}^{(2)} + A_{v2,n}^{(2)} + A_{1,n} \\ C_{v1,n}^{(2)} + C_{v0,n}^{(2)} + C_{1,n} \end{Bmatrix} = \begin{bmatrix} YA11_n & YA12_n \\ YC11_n & YC12_n \end{bmatrix} \begin{Bmatrix} A_{v5,n}^{(2)} \\ C_{v5,n}^{(2)} \end{Bmatrix} + \frac{\mu_s}{\mu_v} \begin{bmatrix} YAS1_n & YAS2_n \\ YCS1_n & YCS2_n \end{bmatrix} \begin{Bmatrix} A_{s1,n}^{(2)} + A_{s2,n}^{(2)} + A_{s0,n}^{(2)} + A_{0,n} \\ C_{s1,n}^{(2)} + C_{s2,n}^{(2)} + C_{s0,n}^{(2)} + C_{0,n} \end{Bmatrix} \tag{30a}$$

$$\begin{Bmatrix} B_{v1,n}^{(2)} + B_{v2,n}^{(2)} + B_{1,n} \\ D_{v1,n}^{(2)} + D_{v0,n}^{(2)} + D_{1,n} \end{Bmatrix} = \begin{bmatrix} YB11_n & YB12_n \\ YD11_n & YD12_n \end{bmatrix} \begin{Bmatrix} B_{v5,n}^{(2)} \\ D_{v5,n}^{(2)} \end{Bmatrix} + \frac{\mu_s}{\mu_v} \begin{bmatrix} YBS1_n & YBS2_n \\ YDS1_n & YDS2_n \end{bmatrix} \begin{Bmatrix} B_{s1,n}^{(2)} + B_{s2,n}^{(2)} + B_{s0,n}^{(2)} + B_{0,n} \\ D_{s1,n}^{(2)} + D_{s2,n}^{(2)} + D_{s0,n}^{(2)} + D_{0,n} \end{Bmatrix} \tag{30b}$$

From Eq (28), we can know unknown coefficients $YA11_n$, $YAS1_n$.

From Eqs (27), (29) and (31), the following equations can be obtained:

$$\begin{Bmatrix} A_{s1,n}^{(2)} + A_{s2,n}^{(2)} + A_{s0,n}^{(2)} + A_{0,n} \\ C_{s1,n}^{(2)} + C_{s2,n}^{(2)} + C_{s0,n}^{(2)} + C_{0,n} \end{Bmatrix} = \begin{bmatrix} EFAA1_n & EFAC1_n \\ EFAA2_n & EFAC2_n \end{bmatrix}^{-1} \begin{bmatrix} RA11_n & RC11_n \\ RA12_n & RC12_n \end{bmatrix}^{-1} \begin{Bmatrix} A_{1,n} \\ C_{1,n} \end{Bmatrix} \tag{31a}$$

$$\begin{Bmatrix} B_{s1,n}^{(2)} + B_{s2,n}^{(2)} + B_{s0,n}^{(2)} + B_{0,n} \\ D_{s1,n}^{(2)} + D_{s2,n}^{(2)} + D_{s0,n}^{(2)} + D_{0,n} \end{Bmatrix} = \begin{bmatrix} EFBB1_n & EFBD1_n \\ EFBB2_n & EFBD2_n \end{bmatrix}^{-1} \begin{bmatrix} RB11_n & RD11_n \\ RB12_n & RD12_n \end{bmatrix}^{-1} \begin{Bmatrix} B_{1,n} \\ D_{1,n} \end{Bmatrix} \tag{31b}$$

Substituting Eq (28) into Eq (30), the unknown coefficients $EFAA1_n$, $RA11_n$ can be obtained.

(2) Enclosed region

Applying the boundary conditions (35), the following equations can be derived:

$$\begin{Bmatrix} A_{v7,l}^{(3)} \\ C_{v7,l}^{(3)} \end{Bmatrix} = \begin{bmatrix} XA11_l & XA12_l \\ XC11_l & XC12_l \end{bmatrix} \begin{Bmatrix} A_{v4,l}^{(3)} \\ C_{v4,l}^{(3)} \end{Bmatrix} \begin{Bmatrix} B_{v7,l}^{(3)} \\ D_{v7,l}^{(3)} \end{Bmatrix} = \begin{bmatrix} XB11_l & XB12_l \\ XD11_l & XD12_l \end{bmatrix} \begin{Bmatrix} B_{v4,l}^{(3)} \\ D_{v4,l}^{(3)} \end{Bmatrix} \tag{32a}$$

$$\begin{Bmatrix} A_{v7,r}^{(4)} \\ C_{v7,r}^{(4)} \end{Bmatrix} = \begin{bmatrix} XA11_r & XA12_r \\ XC11_r & XC12_r \end{bmatrix} \begin{Bmatrix} A_{v4,r}^{(4)} \\ C_{v4,r}^{(4)} \end{Bmatrix} \begin{Bmatrix} B_{v7,r}^{(4)} \\ D_{v7,r}^{(4)} \end{Bmatrix} = \begin{bmatrix} XB11_r & XB12_r \\ XD11_r & XD12_r \end{bmatrix} \begin{Bmatrix} B_{v4,r}^{(4)} \\ D_{v4,r}^{(4)} \end{Bmatrix} \tag{32b}$$

$$\begin{Bmatrix} A_{s6,l}^{(3)} \\ C_{s6,l}^{(3)} \end{Bmatrix} = \begin{bmatrix} XSA11_l & XSA12_l \\ XSC11_l & XSC12_l \end{bmatrix} \begin{Bmatrix} A_{s4,l}^{(3)} \\ C_{s4,l}^{(3)} \end{Bmatrix} \begin{Bmatrix} B_{s6,l}^{(3)} \\ D_{s6,l}^{(3)} \end{Bmatrix} = \begin{bmatrix} XSB11_l & XSB12_l \\ XSD11_l & XSD12_l \end{bmatrix} \begin{Bmatrix} B_{s4,l}^{(3)} \\ D_{s4,l}^{(3)} \end{Bmatrix} \tag{33a}$$

$$\begin{Bmatrix} A_{s6,r}^{(4)} \\ C_{s6,r}^{(4)} \end{Bmatrix} = \begin{bmatrix} XSA11_r & XSA12_r \\ XSC11_r & XSC12_r \end{bmatrix} \begin{Bmatrix} A_{s4,l}^{(4)} \\ C_{s4,l}^{(4)} \end{Bmatrix} \begin{Bmatrix} B_{s6,r}^{(4)} \\ D_{s6,r}^{(4)} \end{Bmatrix}$$
$$= \begin{bmatrix} XSB11_r & XSB12_r \\ XSD11_r & XSD12_r \end{bmatrix} \begin{Bmatrix} B_{s4,l}^{(4)} \\ D_{s4,l}^{(4)} \end{Bmatrix} \tag{33b}$$

Unknown coefficients $XA11_l$, $XB11_r$, $XSA11_l$ and $XSB11_r$ can be easily determined by referring to Eqs (28) and (30).

(3) The auxiliary arc boundary

Applying the boundary conditions $\tau_{rr}^{v(c)} = \tau_{rr}^{v(o)}, \tau_{r\theta}^{v(c)} = \tau_{r\theta}^{v(o)} (r_1 = a, -\delta_1 \ll \theta_1 \ll -\partial_1, \partial_1 \ll \theta_1 \ll \delta_1)$, the following equations can be derived:

$$\begin{Bmatrix} A_{v1,m}^{(1)} + A_{v2,m}^{(1)} + A_{v5,m}^{(1)} + A_{1,m} \\ C_{v1,m}^{(1)} + C_{v2,m}^{(1)} + C_{v5,m}^{(1)} + C_{1,m} \end{Bmatrix} = \begin{bmatrix} WA11_m & WC11_m \\ WA21_m & WC21_m \end{bmatrix} \begin{Bmatrix} A_{v7,m}^{(1)} \\ C_{v7,m}^{(1)} \end{Bmatrix} + \begin{bmatrix} WA12_m & WC12_m \\ WA22_m & WC22_m \end{bmatrix} \begin{Bmatrix} A_{v4,m}^{(1L)} \\ C_{v4,m}^{(1L)} \end{Bmatrix}$$
$$= \begin{bmatrix} WA11_m & WC11_m \\ WA21_m & WC21_m \end{bmatrix} \begin{Bmatrix} A_{v7,m}^{(1)} \\ C_{v7,m}^{(1)} \end{Bmatrix} + \begin{bmatrix} WA12_m & WC12_m \\ WA22_m & WC22_m \end{bmatrix} \begin{Bmatrix} A_{v4,m}^{(1R)} \\ C_{v4,m}^{(1R)} \end{Bmatrix} \tag{34a}$$

$$\begin{Bmatrix} B_{v1,m}^{(1)} + B_{v2,m}^{(1)} + B_{v5,m}^{(1)} + B_{1,m} \\ D_{v1,m}^{(1)} + D_{v2,m}^{(1)} + D_{v5,m}^{(1)} + D_{1,m} \end{Bmatrix} = \begin{bmatrix} WB11_m & WD11_m \\ WB21_m & WD21_m \end{bmatrix} \begin{Bmatrix} B_{v7,m}^{(1)} \\ D_{v7,m}^{(1)} \end{Bmatrix} + \begin{bmatrix} WB12_m & WD12_m \\ WB22_m & WD22_m \end{bmatrix} \begin{Bmatrix} B_{v4,m}^{(1L)} \\ D_{v4,m}^{(1L)} \end{Bmatrix}$$
$$= \begin{bmatrix} WB11_m & WD11_m \\ WB21_m & WD21_m \end{bmatrix} \begin{Bmatrix} B_{v7,m}^{(1)} \\ D_{v7,m}^{(1)} \end{Bmatrix} + \begin{bmatrix} WB12_m & WD12_m \\ WB22_m & WD22_m \end{bmatrix} \begin{Bmatrix} B_{v4,m}^{(1R)} \\ D_{v4,m}^{(1R)} \end{Bmatrix} \tag{34b}$$

Where unknow coefficients $WA11_m$, $WB11_m$ can be easily determined by referring to Eqs (28) and (30).

Applying the boundary conditions $u_r^{v(o)} = u_r^{v(c)}, u_\theta^{v(o)} = u_\theta^{v(c)}, (r_1 = a, -\delta_1 \ll \theta_1 \ll -\partial_1, \partial_1 \ll \theta_1 \ll \delta_1)$, the following equations can be derived:

$$\begin{Bmatrix} A_{v1,m}^{(1)} + A_{v2,m}^{(1)} + A_{v5,m}^{(1)} + A_{1,m} \\ C_{v1,m}^{(1)} + C_{v2,m}^{(1)} + C_{v5,m}^{(1)} + C_{1,m} \end{Bmatrix} = \begin{bmatrix} VA11_m & VC11_m \\ VA21_m & VC21_m \end{bmatrix} \begin{Bmatrix} A_{v7,m}^{(1)} \\ C_{v7,m}^{(1)} \end{Bmatrix} + \begin{bmatrix} VA12_m & VC12_m \\ VA22_m & VC22_m \end{bmatrix} \begin{Bmatrix} A_{v4,m}^{(1L)} \\ C_{v4,m}^{(1L)} \end{Bmatrix}$$
$$= \begin{bmatrix} VA11_m & VC11_m \\ VA21_m & VC21_m \end{bmatrix} \begin{Bmatrix} A_{v7,m}^{(1)} \\ C_{v7,m}^{(1)} \end{Bmatrix} + \begin{bmatrix} VA12_m & VC12_m \\ VA22_m & VC22_m \end{bmatrix} \begin{Bmatrix} A_{v4,m}^{(1R)} \\ C_{v4,m}^{(1R)} \end{Bmatrix} \tag{35a}$$

$$\begin{Bmatrix} B_{v1,m}^{(1)} + B_{v2,m}^{(1)} + B_{v5,m}^{(1)} + B_{1,m} \\ D_{v1,m}^{(1)} + D_{v2,m}^{(1)} + D_{v5,m}^{(1)} + D_{1,m} \end{Bmatrix} = \begin{bmatrix} VB11_m & VD11_m \\ VB21_m & VD21_m \end{bmatrix} \begin{Bmatrix} B_{v7,m}^{(1)} \\ D_{v7,m}^{(1)} \end{Bmatrix} + \begin{bmatrix} VB12_m & VD12_m \\ VB22_m & VD22_m \end{bmatrix} \begin{Bmatrix} B_{v4,m}^{(1L)} \\ D_{v4,m}^{(1L)} \end{Bmatrix}$$
$$= \begin{bmatrix} VB11_m & VD11_m \\ VB21_m & VD21_m \end{bmatrix} \begin{Bmatrix} B_{v7,m}^{(1)} \\ D_{v7,m}^{(1)} \end{Bmatrix} + \begin{bmatrix} VB12_m & VD12_m \\ VB22_m & VD22_m \end{bmatrix} \begin{Bmatrix} B_{v4,m}^{(1R)} \\ D_{v4,m}^{(1R)} \end{Bmatrix} \tag{35b}$$

Combining Eqs. (33)–(35))-(36) and the appropriate coordinate transformation, the following equations can be derived:

$$\sum_{l=0}^{\infty}\begin{Bmatrix} T_{1,V}^{4L(3)}A_{v4,l}^{(3)} \\ T_{4,V}^{4L(3)}C_{v4,l}^{(3)} \end{Bmatrix} = \sum_{n=0}^{\infty}\left(\begin{bmatrix} XHRA1_n & XHRC1_n \\ XHRA2_n & XHRC2_n \end{bmatrix} \begin{Bmatrix} F1_{mn}^{+}(k_{v\alpha}D_{12})A_{1,n} \\ F1_{mn}^{-}(k_{v\beta}D_{12})C_{1,n} \end{Bmatrix} + \begin{bmatrix} WHA1_m + WA12_m & WHC1_m + WC12_m \\ WHA2_m + WA22_m & WHC2_m + WC22_m \end{bmatrix}^{-1} \begin{Bmatrix} F1_{mn}^{+}(k_{v\alpha}D_{12})A_{1,n} \\ F1_{mn}^{-}(k_{v\beta}D_{12})C_{1,n} \end{Bmatrix} \right) \tag{36a}$$

$$\sum_{l=0}^{\infty}\begin{Bmatrix} T_{4,V}^{4L(3)}B_{v4,l}^{(3)} \\ T_{1,V}^{4L(3)}D_{v4,l}^{(3)} \end{Bmatrix} = \sum_{n=0}^{\infty}\left(\begin{bmatrix} XHRB1_n & XHRD1_n \\ XHRB2_n & XHRD2_n \end{bmatrix} \begin{Bmatrix} F1_{mn}^{-}(k_{v\alpha}D_{12})B_{1,n} \\ F1_{mn}^{+}(k_{v\beta}D_{12})D_{1,n} \end{Bmatrix} + \begin{bmatrix} WHB1_m + WB12_m & WHD1_m + WD12_m \\ WHB2_m + WB22_m & WHD2_m + WD22_m \end{bmatrix}^{-1} \begin{Bmatrix} F1_{mn}^{-}(k_{v\alpha}D_{12})B_{1,n} \\ F1_{mn}^{+}(k_{v\beta}D_{12})D_{1,n} \end{Bmatrix} \right) \tag{36b}$$

$$\sum_{r=0}^{\infty}\begin{Bmatrix} T_{1,V}^{4R(3)}A_{v4,l}^{(4)} \\ T_{4,V}^{4R(3)}C_{v4,l}^{(4)} \end{Bmatrix} = \sum_{n=0}^{\infty}\left(\begin{bmatrix} XHRA1_n & XHRC1_n \\ XHRA2_n & XHRC2_n \end{bmatrix} \begin{Bmatrix} F1_{mn}^{+}(k_{v\alpha}D_{12})A_{1,n} \\ F1_{mn}^{-}(k_{v\beta}D_{12})C_{1,n} \end{Bmatrix} + \begin{bmatrix} WHA1_m + WA12_m & WHC1_m + WC12_m \\ WHA2_m + WA22_m & WHC2_m + WC22_m \end{bmatrix}^{-1} \begin{Bmatrix} F1_{mn}^{+}(k_{v\alpha}D_{12})A_{1,n} \\ F1_{mn}^{-}(k_{v\beta}D_{12})C_{1,n} \end{Bmatrix} \right) \tag{37a}$$

$$\sum_{r=0}^{\infty}\begin{Bmatrix} T_{4,V}^{4R(3)}B_{v4,l}^{(3)} \\ T_{1,V}^{4R(3)}D_{v4,l}^{(3)} \end{Bmatrix} = \sum_{n=0}^{\infty}\left(\begin{bmatrix} XHRB1_n & XHRD1_n \\ XHRB2_n & XHRD2_n \end{bmatrix} \begin{Bmatrix} F1_{mn}^{-}(k_{v\alpha}D_{12})B_{1,n} \\ F1_{mn}^{+}(k_{v\beta}D_{12})D_{1,n} \end{Bmatrix} + \begin{bmatrix} WHB1_m + WB12_m & WHD1_m + WD12_m \\ WHB2_m + WB22_m & WHD2_m + WD22_m \end{bmatrix}^{-1} \begin{Bmatrix} F1_{mn}^{-}(k_{v\alpha}D_{12})B_{1,n} \\ F1_{mn}^{+}(k_{v\beta}D_{12})D_{1,n} \end{Bmatrix} \right) \tag{37b}$$

Through the coordinate transformation, and substituting Eqs. (37) and (38) into Eq. (33), the following efficients can be obtained.

$$\begin{Bmatrix} A_{v7,l}^{(3)} \\ C_{v7,l}^{(3)} \end{Bmatrix}, \begin{Bmatrix} B_{v7,l}^{(3)} \\ D_{v7,l}^{(3)} \end{Bmatrix}, \begin{Bmatrix} A_{v7,r}^{(3)} \\ C_{v7,r}^{(3)} \end{Bmatrix}, \begin{Bmatrix} B_{v7,r}^{(3)} \\ D_{v7,r}^{(3)} \end{Bmatrix}$$

Applying the boundary conditions $\tau_{r\theta}^{s(o)} = \tau_{r\theta}^{s(c)}, \tau_{rr}^{s(o)} = \tau_{rr}^{s(c)} (r_1 = a, -\partial_1 \le \theta_1 \le \partial_1)$, the following equations can be derived:

$$\begin{Bmatrix} A_{s1,m}^{(1)} + A_{s2,m}^{(1)} + A_{0,m} \\ C_{s1,m}^{(1)} + C_{s2,m}^{(1)} + C_{0,m} \end{Bmatrix} = \begin{bmatrix} SA11_m & SC11_m \\ SA21_m & SC21_m \end{bmatrix} \begin{Bmatrix} A_{s6,m}^{(1)} \\ C_{s6,m}^{(1)} \end{Bmatrix} + \begin{bmatrix} SA12_m & SC12_m \\ SA22_m & SC22_m \end{bmatrix} \begin{Bmatrix} A_{s4,m}^{(1L)} \\ C_{s4,m}^{(1L)} \end{Bmatrix} \tag{38a}$$

$$\begin{Bmatrix} B_{s1,m}^{(1)} + B_{s2,m}^{(1)} + B_{0,m} \\ D_{s1,m}^{(1)} + D_{s2,m}^{(1)} + D_{0,m} \end{Bmatrix} = \begin{bmatrix} SB11_m & SD11_m \\ SB21_m & SD21_m \end{bmatrix} \begin{Bmatrix} B_{s6,m}^{(1)} \\ D_{s6,m}^{(1)} \end{Bmatrix} + \begin{bmatrix} SB12_m & SD12_m \\ SB22_m & SD22_m \end{bmatrix} \begin{Bmatrix} B_{s4,m}^{(1L)} \\ D_{s4,m}^{(1L)} \end{Bmatrix} \tag{38b}$$

Where $SA11_m$, $SA12_m$ can be easily obtained according to Eqs (28) and (30).

Applying the boundary conditions $u_r^{s(o)} = u_r^{s(c)}, u_r^{s(o)} = u_r^{s(c)} (r_1 = a, -\partial_1 \le \theta_1 \le \partial_1)$, the following equations can be derived:

$$\begin{Bmatrix} A_{s0,m}^{(1)} + A_{s1,m}^{(1)} + A_{s2,m}^{(1)} + A_{0,m} \\ C_{s0,m}^{(1)} + C_{s1,m}^{(1)} + C_{s2,m}^{(1)} + C_{0,m} \end{Bmatrix} = \begin{bmatrix} GA11_m & GC11_m \\ GA21_m & GC21_m \end{bmatrix} \begin{Bmatrix} A_{s6,m}^{(1)} \\ C_{s6,m}^{(1)} \end{Bmatrix} + \begin{bmatrix} GA12_m & GC12_m \\ GA22_m & GC22_m \end{bmatrix} \begin{Bmatrix} A_{s4,m}^{(1L)} \\ C_{s4,m}^{(1L)} \end{Bmatrix} \tag{39a}$$

$$\begin{Bmatrix} B_{s0,m}^{(1)} + B_{s1,m}^{(1)} + B_{s2,m}^{(1)} + B_{0,m} \\ D_{s0,m}^{(1)} + D_{s1,m}^{(1)} + D_{s2,m}^{(1)} + D_{0,m} \end{Bmatrix} = \begin{bmatrix} GB11_m & GD11_m \\ GB21_m & GD21_m \end{bmatrix} \begin{Bmatrix} B_{s6,m}^{(1)} \\ D_{s6,m}^{(1)} \end{Bmatrix} + \begin{bmatrix} GB12_m & GD12_m \\ GB22_m & GD22_m \end{bmatrix} \begin{Bmatrix} B_{s4,m}^{(1L)} \\ D_{s4,m}^{(1L)} \end{Bmatrix} \tag{39b}$$

Where unknown coefficients $GA11_m$, $GA12_m$ can be easily determined by referring to Eqs (28) and (30).

Through the coordinate transformation, the following equations can be derived:

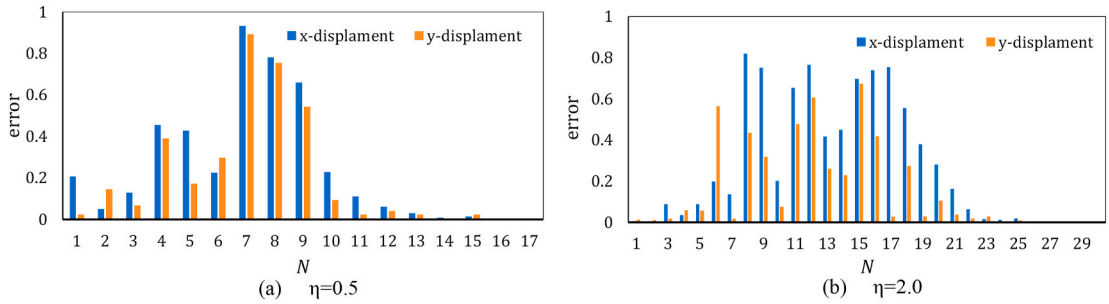

Fig. 4. The convergence of series solution with the truncation number N_c of terms.

$$\sum_{l=0}^{\infty}\begin{Bmatrix} T_{1,S}^{4L(3)}A_{s4,l}^{(3)} \\ T_{4,S}^{4L(3)}C_{s4,l}^{(3)} \end{Bmatrix} = \sum_{l=0}^{\infty}\begin{Bmatrix} T_{1,S}^{4R(3)}A_{s4,r}^{(3)} \\ T_{4,S}^{4R(3)}C_{s4,r}^{(3)} \end{Bmatrix} = \sum_{n=0}^{\infty}\begin{bmatrix} UA1_m & UC1_m \\ UA2_m & UC2_m \end{bmatrix}\begin{Bmatrix} F1_{mn}^{+}(k_{v\alpha}D_{12})A_{1,n} \\ F1_{mn}^{-}(k_{v\beta}D_{12})C_{1,n} \end{Bmatrix} \tag{40a}$$

$$\sum_{l=0}^{\infty}\begin{Bmatrix} T_{1,S}^{4L(3)}B_{s4,l}^{(3)} \\ T_{4,S}^{4L(3)}D_{s4,l}^{(3)} \end{Bmatrix} = \sum_{l=0}^{\infty}\begin{Bmatrix} T_{1,S}^{4R(3)}B_{s4,r}^{(3)} \\ T_{4,S}^{4R(3)}D_{s4,r}^{(3)} \end{Bmatrix} = \sum_{n=0}^{\infty}\begin{bmatrix} UB1_m & UD1_m \\ UB2_m & UD2_m \end{bmatrix}\begin{Bmatrix} F1_{mn}^{-}(k_{v\alpha}D_{12})B_{1,n} \\ F1_{mn}^{+}(k_{v\beta}D_{12})D_{1,n} \end{Bmatrix} \tag{40b}$$

Where $UA1_m$, $UB1_m$ can be easily obtained by coefficients derived above. Next, the surface displacements can be calculated by the following expressions:

For $r_2 = R + H$:

$$\begin{aligned}
\begin{Bmatrix} u_r(r_2,\theta_2) \\ u_\theta(r_2,\theta_2) \end{Bmatrix} &= \frac{1}{R+H}\sum_{n=0}^{\infty}\begin{bmatrix} I_{11}^{v_o(1)}(n,R+H) & I_{12}^{v_o(1)+}(n,R+H) \\ I_{21}^{v_o(1)-}(n,R+H) & I_{22}^{v_o(1)}(n,R+H) \end{bmatrix}\begin{Bmatrix} A_{v1,n}^{(2)}+A_{v2,n}^{(2)}+A_{1,n} \\ C_{v1,n}^{(2)}+C_{v2,n}^{(2)}+C_{1,n} \end{Bmatrix}\begin{Bmatrix} \cos n\theta_2 \\ \sin n\theta_2 \end{Bmatrix} \\
&+\frac{1}{R+H}\sum_{n=0}^{\infty}\begin{bmatrix} I_{11}^{v_o(3)}(n,R+H) & I_{12}^{v_o(3)+}(n,R+H) \\ I_{21}^{v_o(3)-}(n,R+H) & I_{22}^{v_o(3)}(n,R+H) \end{bmatrix}\begin{Bmatrix} A_{v5,n}^{(2)} \\ C_{v5,n}^{(2)} \end{Bmatrix}\begin{Bmatrix} \cos n\theta_2 \\ \sin n\theta_2 \end{Bmatrix} \\
&+\frac{1}{R+H}\sum_{n=0}^{\infty}\begin{bmatrix} I_{11}^{v_o(1)}(n,R+H) & I_{12}^{v_o(1)-}(n,R+H) \\ I_{21}^{v_o(1)+}(n,R+H) & I_{22}^{v_o(1)}(n,R+H) \end{bmatrix}\begin{Bmatrix} B_{v1,n}^{(2)}+B_{v2,n}^{(2)}+B_{1,n} \\ D_{v1,n}^{(2)}+D_{v2,n}^{(2)}+D_{1,n} \end{Bmatrix}\begin{Bmatrix} \sin n\theta_2 \\ \cos n\theta_2 \end{Bmatrix} \\
&+\frac{1}{R+H}\sum_{n=0}^{\infty}\begin{bmatrix} I_{11}^{v_o(3)}(n,R+H) & I_{12}^{v_o(3)-}(n,R+H) \\ I_{21}^{v_o(3)+}(n,R+H) & I_{22}^{v_o(3)}(n,R+H) \end{bmatrix}\begin{Bmatrix} B_{v5,n}^{(2)} \\ D_{v5,n}^{(2)} \end{Bmatrix}\begin{Bmatrix} \sin n\theta_2 \\ \cos n\theta_2 \end{Bmatrix}
\end{aligned} \tag{41}$$

For $r_3 = R_3$, $-\delta_3 \le \theta_3 \le 0$

$$\begin{aligned}
\begin{Bmatrix} u_r^{v(L)}(r_3,\theta_3) \\ u_\theta^{v(L)}(r_3,\theta_3) \end{Bmatrix} &= \frac{1}{R_3}\sum_{l=0}^{\infty}\begin{bmatrix} I_{11}^{1*(1)}(l,R_3) & I_{12}^{1*(1)+}(l,R_3) \\ I_{21}^{1*(1)-}(l,R_3) & I_{22}^{1*(1)}(l,R_3) \end{bmatrix}\begin{Bmatrix} A_{v7,l}^{(3)} \\ C_{v7,l}^{(3)} \end{Bmatrix}\begin{Bmatrix} \cos l\theta_3 \\ \sin l\theta_3 \end{Bmatrix} \\
&+\frac{1}{R_3}\sum_{l=0}^{\infty}\begin{bmatrix} I_{11}^{1*(3)}(l,R_3) & I_{12}^{1*(3)+}(l,R_3) \\ I_{21}^{1*(3)-}(l,R_3) & I_{22}^{1*(3)}(l,R_3) \end{bmatrix}\begin{Bmatrix} A_{v4,l}^{(3)} \\ C_{v4,l}^{(3)} \end{Bmatrix}\begin{Bmatrix} \cos l\theta_3 \\ \sin l\theta_3 \end{Bmatrix}
\end{aligned} \tag{42}$$

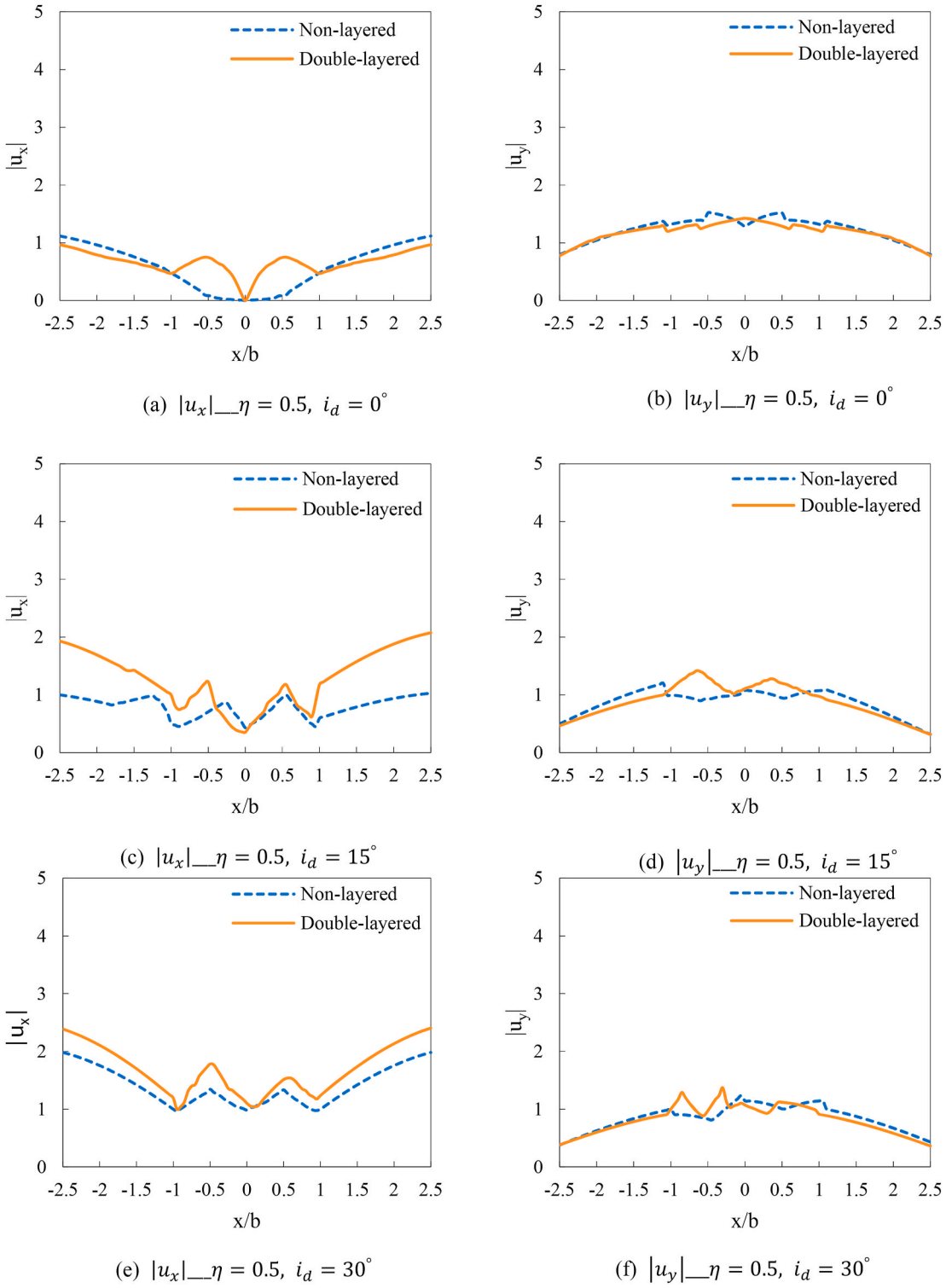

Fig. 5. Difference of displacement amplitudes between Non-layered case and Double-layered case (η = 0.5).

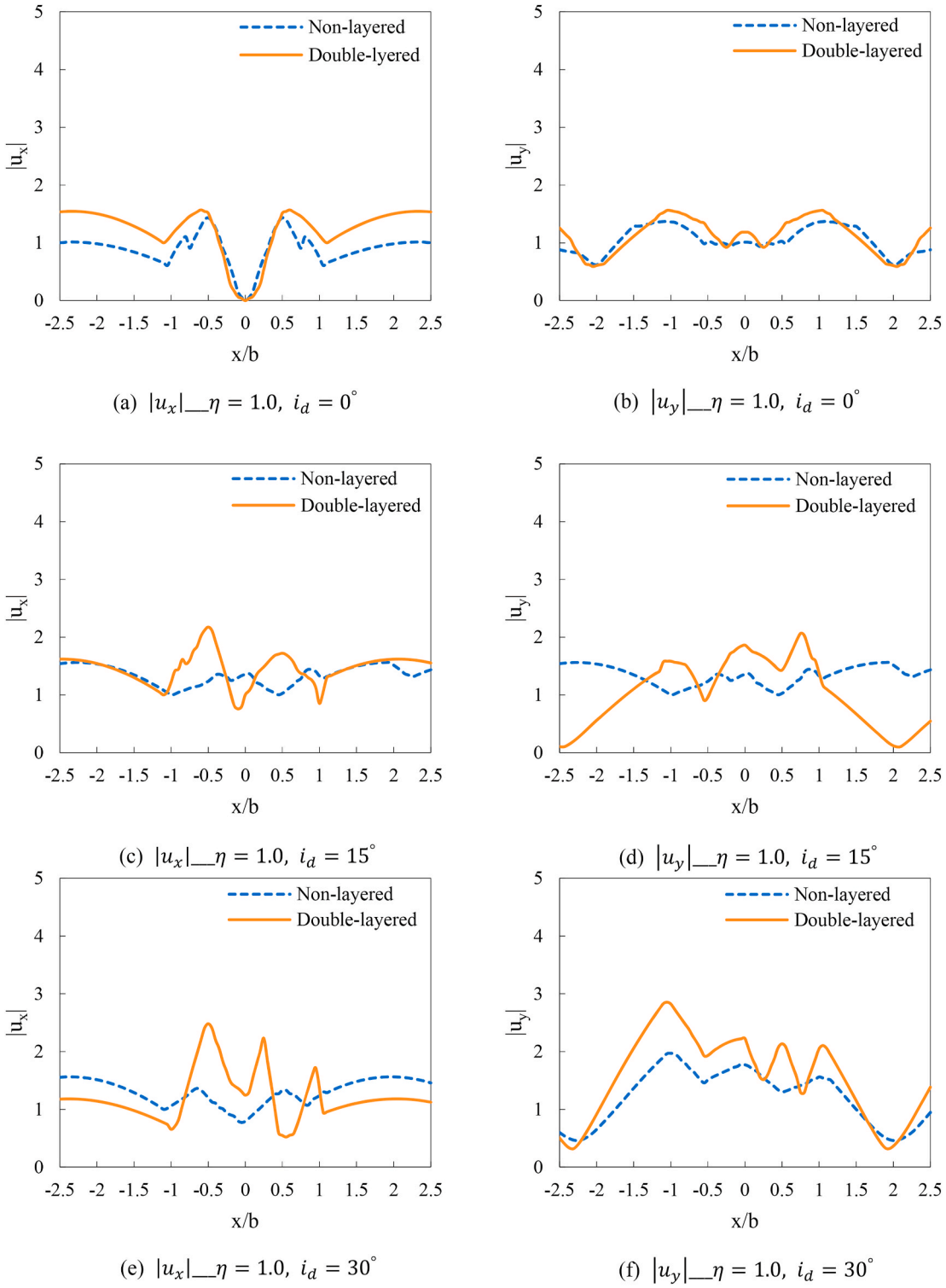

(a) $|u_x|\_\_\eta = 1.0,\ i_d = 0^\circ$ (b) $|u_y|\_\_\eta = 1.0,\ i_d = 0^\circ$

(c) $|u_x|\_\_\eta = 1.0,\ i_d = 15^\circ$ (d) $|u_y|\_\_\eta = 1.0,\ i_d = 15^\circ$

(e) $|u_x|\_\_\eta = 1.0,\ i_d = 30^\circ$ (f) $|u_y|\_\_\eta = 1.0,\ i_d = 30^\circ$

Fig. 6. Difference of displacement amplitudes between Non-layered case and Double-layered case (η = 1.0).

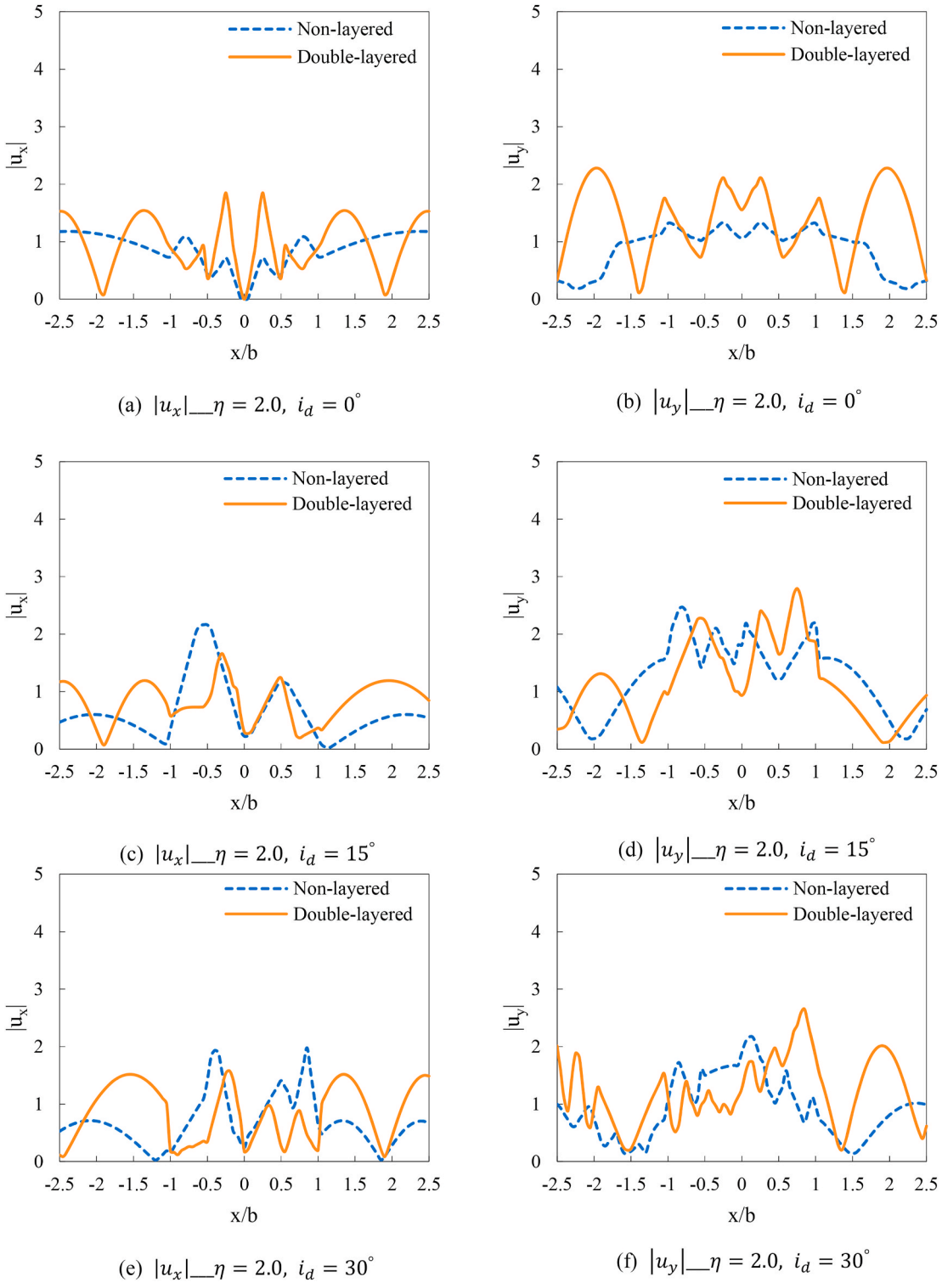

Fig. 7. Difference of displacement amplitudes between Non-layered case and Double-layered case (η = 2.0).

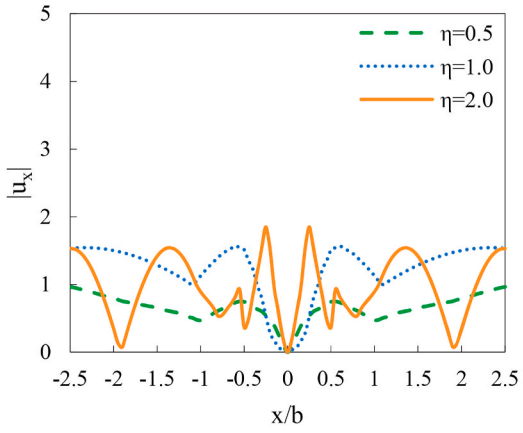

(a) x-displacement amplitudes for $i_d = 0^\circ$

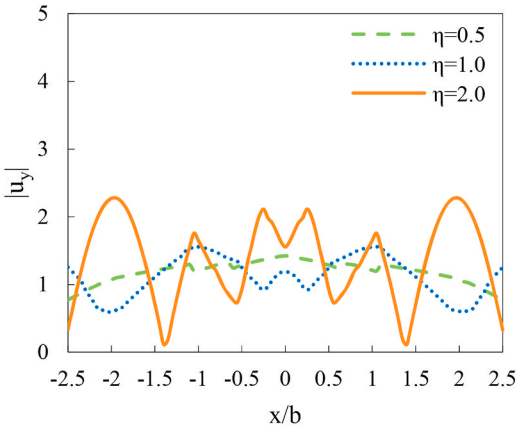

(b) y-displacement amplitudes for $i_d = 0^\circ$

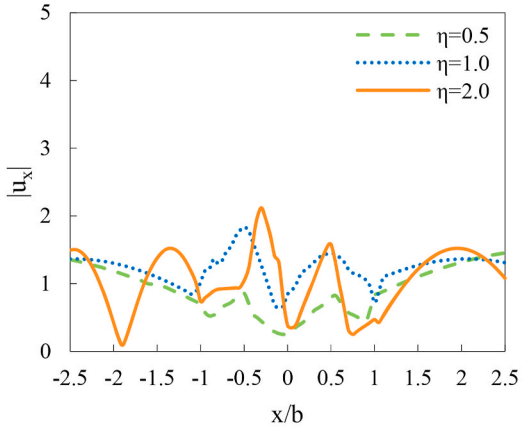

(c) x-displacement amplitudes for $i_d = 15^\circ$

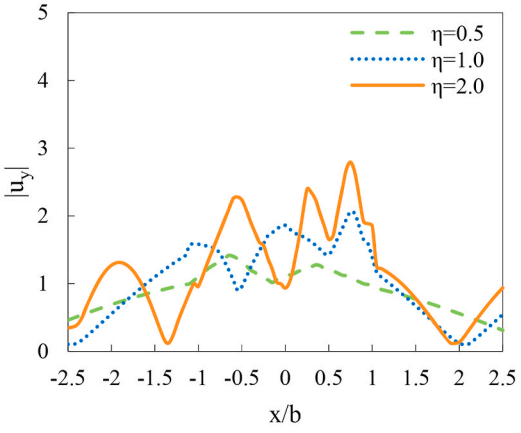

(d) y-displacement amplitudes for $i_d = 15^\circ$

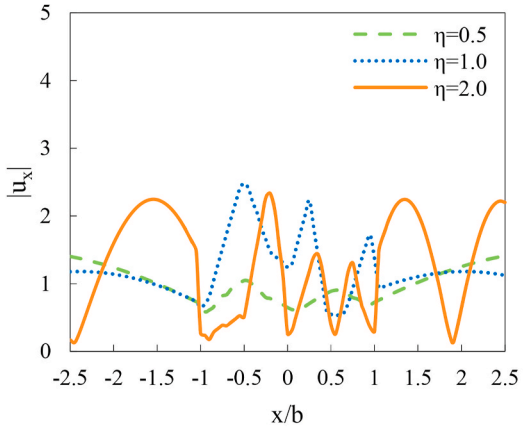

(e) x-displacement amplitudes for $i_d = 30^\circ$

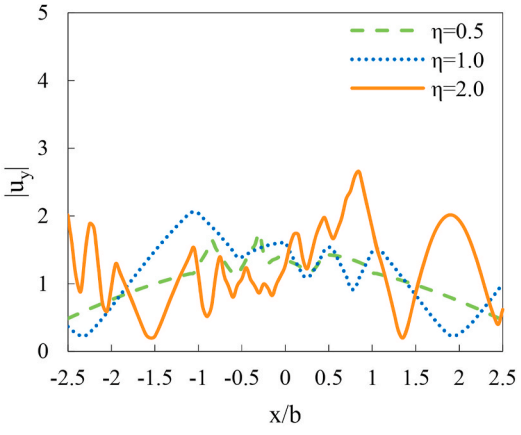

(f) y-displacement amplitudes for $i_d = 30^\circ$

Fig. 8. Comparisons of displacement amplitudes among different frequency.

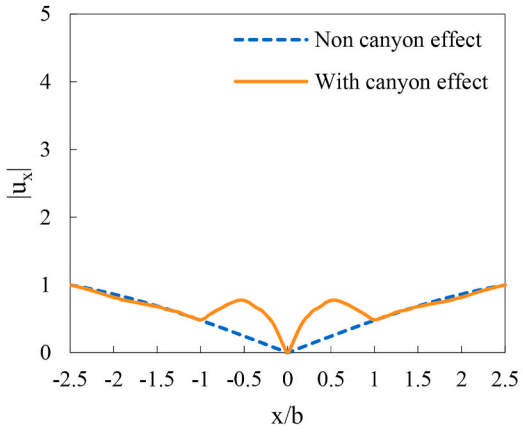

(a) x-displacement amplitudes for $\eta = 0.5$

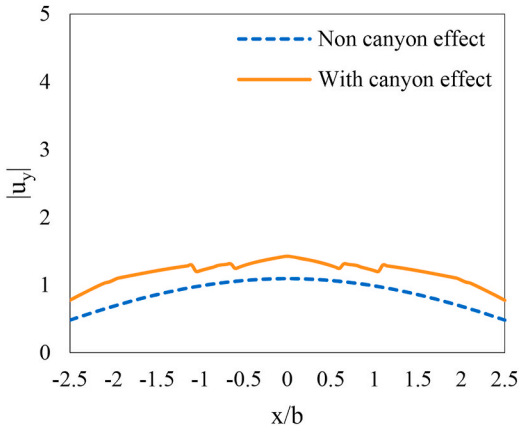

(b) y-displacement amplitudes for $\eta = 0.5$

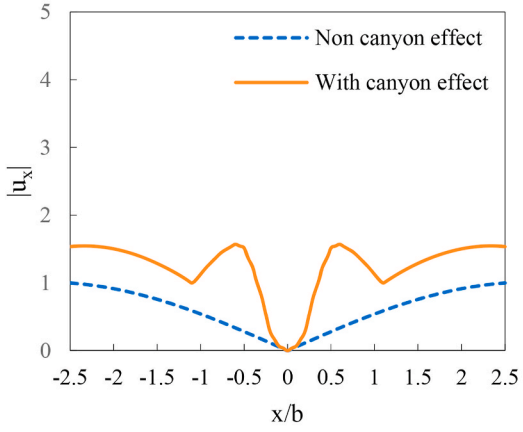

(c) x-displacement amplitudes for $\eta = 1.0$

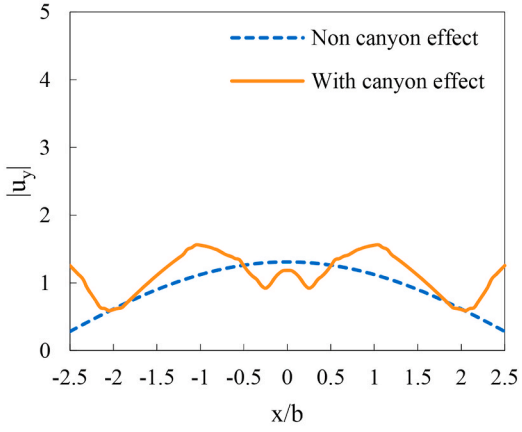

(d) y-displacement amplitudes for $\eta = 1.0$

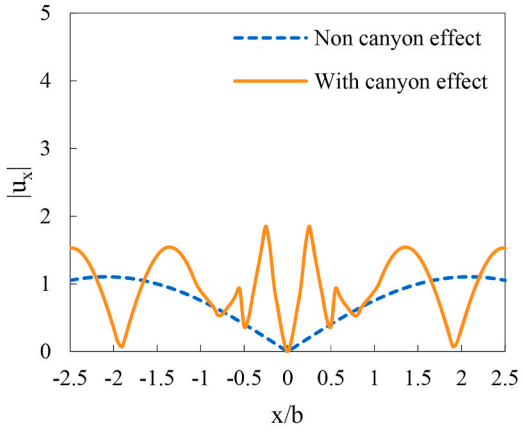

(e) x-displacement amplitudes for $\eta = 2.0$

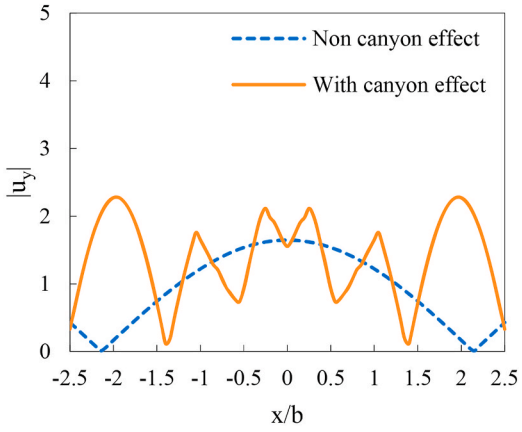

(f) y-displacement amplitudes for $\eta = 2.0$

Fig. 9. Comparisons of displacement amplitudes between the case of no canyon and the case with canyon.

For $r_4 = R_4$, $-\delta_4 \le \theta_4 \le 0$

$$\begin{Bmatrix} u_r^{v(R)}(r_4,\theta_4) \\ u_\theta^{v(R)}(r_4,\theta_4) \end{Bmatrix} = \frac{1}{R_4}\sum_{r=0}^{\infty}\begin{bmatrix} I_{11}^{1*(1)}(r,R_4) & I_{12}^{1*(1)+}(r,R_4) \\ I_{21}^{1*(1)-}(r,R_4) & I_{22}^{1*(1)}(r,R_4) \end{bmatrix}\begin{Bmatrix} A_{v7,r}^{(4)} \\ C_{v7,r}^{(4)} \end{Bmatrix}\begin{Bmatrix} \cos r\theta_4 \\ \sin r\theta_4 \end{Bmatrix}$$
$$+\frac{1}{R_4}\sum_{r=0}^{\infty}\begin{bmatrix} I_{11}^{1*(3)}(r,R_4) & I_{12}^{1*(3)+}(r,R_4) \\ I_{21}^{1*(3)-}(r,R_4) & I_{22}^{1*(3)}(r,R_4) \end{bmatrix}\begin{Bmatrix} A_{v4,r}^{(4)} \\ C_{v4,r}^{(4)} \end{Bmatrix}\begin{Bmatrix} \cos r\theta_4 \\ \sin r\theta_4 \end{Bmatrix}$$
$$+\frac{1}{R_4}\sum_{r=0}^{\infty}\begin{bmatrix} I_{11}^{1*(1)}(r,R_4) & I_{12}^{1*(1)-}(r,R_4) \\ I_{21}^{1*(1)+}(r,R_4) & I_{22}^{1*(1)}(r,R_4) \end{bmatrix}\begin{Bmatrix} B_{v7,r}^{(4)} \\ D_{v7,r}^{(4)} \end{Bmatrix}\begin{Bmatrix} \sin r\theta_4 \\ \cos r\theta_4 \end{Bmatrix}$$
$$\frac{1}{R_4}\sum_{r=0}^{\infty}\begin{bmatrix} I_{11}^{1*(1)}(r,R_4) & I_{12}^{1*(1)-}(r,R_4) \\ I_{21}^{1*(1)+}(r,R_4) & I_{22}^{1*(1)}(r,R_4) \end{bmatrix}\begin{Bmatrix} B_{v7,r}^{(4)} \\ D_{v7,r}^{(4)} \end{Bmatrix}\begin{Bmatrix} \sin r\theta_4 \\ \cos r\theta_4 \end{Bmatrix} \quad (43)$$

For $r_3 = R_3$, $0 \le \theta_3 \le \delta_3$

$$\begin{Bmatrix} u_r^{s(L)}(r_3,\theta_3) \\ u_\theta^{s(L)}(r_3,\theta_3) \end{Bmatrix}$$
$$= \frac{1}{R_3}\sum_{l=0}^{\infty}\begin{bmatrix} I_{11}^{2*(1)}(l,R_3) & I_{12}^{2*(1)+}(l,R_3) \\ I_{21}^{2*(1)-}(l,R_3) & I_{22}^{2*(1)}(l,R_3) \end{bmatrix}\begin{Bmatrix} A_{s6,l}^{(3)} \\ C_{s6,l}^{(3)} \end{Bmatrix}\begin{Bmatrix} \cos l\theta_3 \\ \sin l\theta_3 \end{Bmatrix} \quad (44)$$
$$+\frac{1}{R_3}\sum_{l=0}^{\infty}\begin{bmatrix} I_{11}^{2*(3)}(l,R_3) & I_{12}^{2*(3)+}(l,R_3) \\ I_{21}^{2*(3)-}(l,R_3) & I_{22}^{2*(3)}(l,R_3) \end{bmatrix}\begin{Bmatrix} A_{s4,l}^{(3)} \\ C_{s4,l}^{(3)} \end{Bmatrix}\begin{Bmatrix} \cos l\theta_3 \\ \sin l\theta_3 \end{Bmatrix}$$
$$+\frac{1}{R_3}\sum_{l=0}^{\infty}\begin{bmatrix} I_{11}^{2*(1)}(l,R_3) & I_{12}^{2*(1)-}(l,R_3) \\ I_{21}^{2*(1)+}(l,R_3) & I_{22}^{2*(1)}(l,R_3) \end{bmatrix}\begin{Bmatrix} B_{s6,l}^{(3)} \\ D_{s6,l}^{(3)} \end{Bmatrix}\begin{Bmatrix} \sin l\theta_3 \\ \cos l\theta_3 \end{Bmatrix}$$
$$+\frac{1}{R_3}\sum_{l=0}^{\infty}\begin{bmatrix} I_{11}^{2*(3)}(l,R_3) & I_{12}^{2*(3)-}(l,R_3) \\ I_{21}^{2*(3)+}(l,R_3) & I_{22}^{2*(3)}(l,R_3) \end{bmatrix}\begin{Bmatrix} B_{s4,l}^{(3)} \\ D_{s4,l}^{(3)} \end{Bmatrix}\begin{Bmatrix} \sin l\theta_3 \\ \cos l\theta_3 \end{Bmatrix}$$

For $r_4 = R_4$, $0 \le \theta_4 \le \delta_4$

$$\begin{Bmatrix} u_r^{s(R)}(r_4,\theta_4) \\ u_\theta^{s(R)}(r_4,\theta_4) \end{Bmatrix}$$
$$= \frac{1}{R_4}\sum_{r=0}^{\infty}\begin{bmatrix} I_{11}^{2*(1)}(r,R_4) & I_{12}^{2*(1)+}(r,R_4) \\ I_{21}^{2*(1)-}(r,R_4) & I_{22}^{2*(1)}(r,R_4) \end{bmatrix}\begin{Bmatrix} A_{s6,r}^{(4)} \\ C_{s6,r}^{(4)} \end{Bmatrix}\begin{Bmatrix} \cos r\theta_4 \\ \sin r\theta_4 \end{Bmatrix} \quad (45)$$
$$+\frac{1}{R_4}\sum_{r=0}^{\infty}\begin{bmatrix} I_{11}^{2*(3)}(r,R_4) & I_{12}^{2*(3)+}(r,R_4) \\ I_{21}^{2*(3)-}(r,R_4) & I_{22}^{2*(3)}(r,R_4) \end{bmatrix}\begin{Bmatrix} A_{s4,r}^{(4)} \\ C_{s4,r}^{(4)} \end{Bmatrix}\begin{Bmatrix} \cos r\theta_4 \\ \sin r\theta_4 \end{Bmatrix}$$
$$+\frac{1}{R_4}\sum_{r=0}^{\infty}\begin{bmatrix} I_{11}^{2*(1)}(r,R_4) & I_{12}^{2*(1)-}(r,R_4) \\ I_{21}^{2*(1)+}(r,R_4) & I_{22}^{2*(1)}(r,R_4) \end{bmatrix}\begin{Bmatrix} B_{s6,r}^{(4)} \\ D_{s6,r}^{(4)} \end{Bmatrix}\begin{Bmatrix} \sin r\theta_4 \\ \cos r\theta_4 \end{Bmatrix}$$
$$+\frac{1}{R_4}\sum_{r=0}^{\infty}\begin{bmatrix} I_{11}^{2*(3)}(r,R_4) & I_{12}^{2*(3)-}(r,R_4) \\ I_{21}^{2*(3)+}(r,R_4) & I_{22}^{2*(3)}(r,R_4) \end{bmatrix}\begin{Bmatrix} B_{s4,r}^{(4)} \\ D_{s4,r}^{(4)} \end{Bmatrix}\begin{Bmatrix} \sin r\theta_4 \\ \cos zr\theta_4 \end{Bmatrix}$$

3. Numerical analysis

Numerical analysis is further conducted on the amplification patterns of layered V-shaped canyon of the second stratification type with different parameters. The series solutions of wave functions are applied in this study. More specifically, this study focuses on the study on the behaviors of displacement amplitudes between layered V-shaped canyon of the second stratification type model and non-layered model, and the effect of symmetrical V-shaped canyon with the second stratification type on displacement amplifications.

3.1. Convergence and accuracy of serious solution

Numerical analysis can be used to simulate the topography conditions. The accuracy and convergence are necessary precondition for adopting numerical solution to analyze one model. Consequently, the infinite series of the unknown coefficient solutions need to be truncated for numerical analysis. In this manuscript, we can find that the accuracy and convergence of the results can be influenced by some certain parameters physically or mathematically. The key parameters controlling the accuracy and convergence of the series solution are briefly discussed as follow.

Firstly, the wave velocity contrast (β_v/β_s) between upper-layer (layer-V) and lower-layer (layer-S) is a key factor controlling the accuracy and convergence of the results. By comparing different β_v/β_s, we can find that the requirement of convergence becomes more severe with enlargement of the wave velocity contrast. In the numerical example of this section, the wave velocity contrast ($\beta_v/\beta_s = 2710/2881$) is set as 0.94. Furthermore, it is well known that the seismic wave velocity depends on the physical properties of soil medium. In other words, the greater difference in physical properties between layer-V and layer-S can lead to more difficult controlling the convergence and the accuracy. That is because greater difference in physical properties will causes easier the singularity of coefficients matrix mathematically, which is main reason causing the unstable series solution.

Secondly, the incidence frequency of the elastic wave plays a decisive role in controlling the accuracy of the proposed computational scheme as well. Generally, the higher incident frequency η, the larger the truncation number needed for convergence. Supposing the series is truncated by the finite number of N. Fig. 4 presents the variation of error with the truncation number N, where Fig. 4 (a) is for the incident frequency $\eta = 0.5$ and Fig. 4 (b) for $\eta = 2.0$. As to $\eta = 0.5$, when the truncation number $N \ge 17$, the error is in within the range of accuracy, the convergence number N_c for the incident frequency of 0.5 is 17; while for $\eta = 2.0$, which is higher incident frequency, the convergence number N_c is 30.

3.2. The numerical example

The displacement u at any point of the half-plane with the canyon can be calculated based on the given solution.

The displacements components computed here in cylindrical coordinates are related to the wave potentials by the following equations:

$$\text{Radial: } u_r = \frac{\partial \phi}{\partial r} + \frac{1}{r}\frac{\partial \psi}{\partial \theta} \quad (46a)$$

Table 1
The material parameters.

Material parameters	ρ (kg/m^3)	μ (Mpa)	λ (Mpa)	ν
Layer-V	2450	18	18	0.25
Layer-S	2650	22	22	0.25

(a) The diagram of this paper (b) The diagram of Ref. [40]

Fig. 10. The comparison between this paper and Ref. [40].

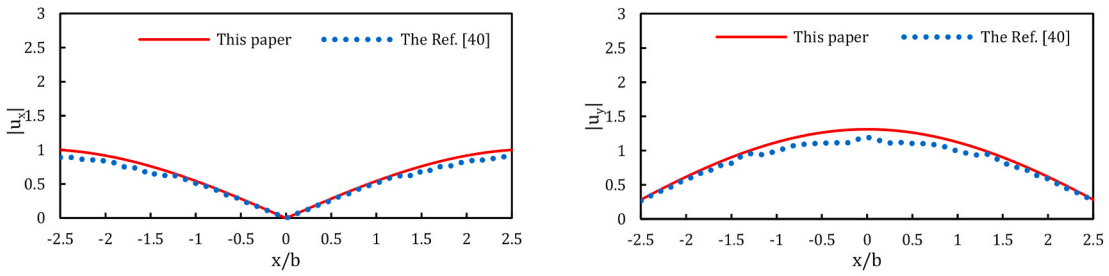

(a) The x-displacement amplitudes (b) The y-displacement amplitudes

Fig. 11. The displacement amplitudes compared with those of Ref. [40] for $\eta = 1.0$.

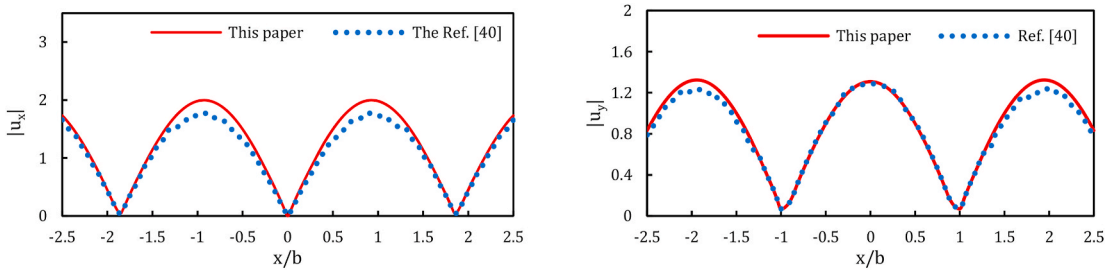

(a) The x-displacement amplitudes (b) The y-displacement amplitudes

Fig. 12. The displacement amplitudes compared with those of Ref. [40] for $\eta = 4.0$.

Angular: $u_\theta = \frac{1}{r}\frac{\partial \phi}{\partial \theta} - \frac{\partial \psi}{\partial r}$ (46b)

Eq. (103) can also be transformed to rectangular components u_x, u_y by

$$\begin{pmatrix} u_x \\ u_y \end{pmatrix} = \begin{bmatrix} \cos\theta & -\sin\theta \\ \sin\theta & \cos\theta \end{bmatrix} \begin{pmatrix} u_r \\ u_\theta \end{pmatrix} \quad (47)$$

As before, the displacements amplitudes are given as:

$$\begin{cases} |u_x| = \sqrt{Real(u_x)^2 + Imag(u_x)^2} \\ |u_y| = \sqrt{Real(u_y)^2 + Imag(u_y)^2} \end{cases} \quad (48)$$

where Real(.) and Imag(.) denote the real and imaginary part of the complex argument. Using the notation of Trifunac [27], the following dimensionless frequency η is defined, as the ratio of the canyon width to

Table 2
Expressions of displacement in Ref. [40].

Expressions of displacement reflection and projection coefficients on the layer-interface	
Coefficients	Formulas
R_{psvp}	$-[2\eta_{\alpha 1}(ab + cd\eta_{\alpha 2}\eta_{\beta 2})p(\alpha_1/\beta_1)]/D$
T_{pp}	$[2\rho_1\eta_{\alpha 1}F(\alpha_1/\alpha_2)]/D$
T_{psv}	$[(b\eta_{\beta 1} - c\eta_{\beta 2})E - (a + d\eta_{\alpha 2}\eta_1)Gp^2]/D$
$a = \rho_2(1 - 2\beta_2^2p^2) - \rho_1(1 - 2\beta_2^2p^2)$	$E = b\eta_{\alpha 1} + c\eta_{\alpha 2}$
$b = \rho_2(1 - 2\beta_2^2p^2) + 2\rho_1\beta_1^2p^2$	$F = b\eta_{\beta 1} + c\eta_{\beta 2}$
$c = \rho_2(1 - 2\beta_1^2p^2) + 2\rho_2\beta_2^2p^2$	$G = a - d\eta_{\alpha 1}\eta_{\beta 2}$
$d = 2(\rho_2\beta_2^2 - \rho_1\beta_1^2)$	$D = EF + GHp^2$
	$A = [(1/\beta^2) - 2p^2]^2 + 4p^2\eta_\alpha\eta_\beta$
	$\eta_c = \sqrt{\frac{1}{c^2} - p^2}, c = \alpha_1, \alpha_2, \beta_1, \beta_2$
Expressions of displacement reflection coefficients on the surface	
$R_{pp}^F = \frac{A_2}{A_1} = \frac{4\beta^4p^2\frac{\cos i_s}{\alpha\beta} - (1 - 2\beta^2p^2)^2}{4\beta^4p^2\frac{\cos i_s}{\alpha\beta} + (1 - 2\beta^2p^2)^2}$	$R_{psv}^F = \frac{B}{A_1} = \frac{-4\beta^4p^2\frac{\cos i_s}{\alpha\beta}(1 - 2\beta^2p^2)^2}{4\beta^4p^2\frac{\cos i_s}{\alpha\beta} + (1 - 2\beta^2p^2)^2}$
$R_{svsv}^F = \frac{B}{A} = \frac{4p^2\frac{\cos i_s \cos i_p}{\alpha\beta} - \left(\frac{1}{\beta^2} - 2p^2\right)^2}{4p^2\frac{\cos i_s \cos i_p}{\alpha\beta} + \left(\frac{1}{\beta^2} - 2p^2\right)^2}$	$R_{svp}^F = \frac{C}{A} = \frac{4p\frac{\cos i_s}{\beta} - \left(\frac{1}{\beta^2} - 2p^2\right)^2}{4p^2\frac{\cos i_s \cos i_p}{\alpha\beta} + \left(\frac{1}{\beta^2} - 2p^2\right)^2}$

the incident wavelength:

$$\eta = \frac{\omega a}{\pi \beta_s} = \frac{2fa_o}{\beta_s} = \frac{k_{s\beta} a_o}{\pi} = \frac{2a_o}{\lambda_s \beta} \tag{49}$$

where the parameters a_0, ω, β_s are defined as before; f = ω/2π is the cyclic frequency in Hz and $\lambda_{s\beta}$ is the wavelength of the shear wave in the half-plane. In the following calculation, Poisson ratios for medium of layer-V and Layer-S are taken as 0.25, i.e., α = 1.732β for the two media.

In the calculation, the radius (R, R_3 and R_4) of the big circular arc that respectively simulates the flat ground and canyon surface are taken a reasonable large value (e.g.100*a,* 50*a,* 20*a* etc), which aim to achieve simultaneously the computational convergence, stability and efficiency. We assume the half-width of the canyon, *b*, is half of the surface length an of the canyon *a*, i.e. *a* = *2b*, the ratio of the depth *h* to the half-width *b* of the canyon is 1.732. The depth *h* of the canyon is a nonnegative number, and the half-width *b* and the depth *h* are set to be 250 m and 433 m, respectively, i.e. *b* = 250 m, *h* = 433 m. The thickness of layer V, *H*, is taken as half of the canyon depth for the convenience, i.e. *H* = *h*/2 = 216.5 m (The assumption is only used for the following numerical example, and the H in the theoretical solution above in section 2.3 is arbitrary). The shear moduli μ_v and μ_s of Layer-V and Layer-S are set to be 18Mpa and 22Mpa, respectively, i.e. μ_v = 18Mpa, μ_s = 22Mpa.

Fig. 5 to Fig. 7 show the displacement amplitudes of the V-shaped canyon with non-layered ($\mu_v = \mu_s$ = 22Mpa) and double-layered (μ_v = 18Mpa, μ_s = 22Mpa) for incident P wave with low (η = 0.5), medium (η = 1.0) and high (η = 2.0) frequencies, at three different incident angles 0, π/12 and π/6 to study the effect of inhomogeneous medium on the scattering of P wave incident V-shaped canyon.

From Fig. 5, we can find that under double-layered case, the x-component displacement amplitudes on the ground almost are larger than that of the homogeneous medium at low frequency, especially the ground of canyon (|*x*/*b*|<1.0). It indicates that inhomogeneous medium has magnified effect on response of scattering of P wave. Furthermore, higher y-component displacement amplitudes and more intensive fluctuation on the ground of canyon (|*x*/*b*|<1.0) than one on the flat ground (|*x*/*b*|>1.0) illustrate further that layered effect has exert influence upon response of ground displacements on the canyon. In contrast to the y-component displacement amplitudes, the *x*-component counterparts are smaller at the ground of canyon than the horizontal ground surface, and the minimum value are located at near the canyon bottom (|*x*/*b*| = 0). Fig. 6 shows that at medium frequency, the trend of fluctuation of both the *x*- and *y*-component displacement amplitudes are relatively more intensive at the ground of canyon than those at the horizontal ground surface. Meanwhile, we can know from the results that both the maximum and the minimum values of *x*-component displacement amplitudes appear on the ground surface of the canyon (−1.0< *x*/*b* < 0), and the *y*-component displacement amplitudes on the ground of canyon almost are higher than that of the non-layered medium. These provide further evidence that layered effect will emerge greater affection on the properties of ground motion due to existence of canyon. Fig. 7 shows the case of high frequency, both the *x*- and *y*-component displacement amplitudes are the highest for ether double-layered sequence or non-layered sequence, and the surface displacements at double-layered model fluctuate greater comparing with those at the non-layered model. Moreover, both the *x*- and *y*-component displacement amplitudes present more significant difference between non-layered model and homogeneous medium at high frequency. The above-mentioned results prove that the layered effect on scattering of incident waves cannot be neglected as researching the properties of ground motion. Therefore, it may not be appropriate to analyze surface displacements of double-layered V-shaped canyon by non-layered model. In addition, the study on the double-layered model is necessary for earthquake simulation and seismic risk assessment.

Fig. 8 gives the variations of the displacement amplitudes on the ground surface for the incident frequencies of 0.5, 1.0 and 2.0 under the incident angle is 0, pi/12, pi/6. We can see from the results that both the horizontal and vertical ground surface displacement amplitudes show greater fluctuation and increase gradually with the increase of frequency. In addition, the displacement amplitudes on the plat ground surface become more intensive as increasing incident *η*. Therefore, compared with low incident frequency, incident wave with the high frequency potentially results in enlargement of the displacement amplitudes on the ground surface and more intensive ground motion under the large incident angle.

Fig. 9 depicts comparisons of displacement amplitudes on the ground surface between the case of no case canyon effect and the case with canyon effect. As is shown in Fig. 9, more significant difference of both x- and y-component displacement amplitudes on the ground surface are presented between the case of no canyon effect and the case with canyon effect as increase of incident frequency under the incident angle is 0. Moreover, the displacement amplitudes with canyon effect show more intensive fluctuation than the case of no canyon, especially at high incident frequency (η = 2.0). Furthermore, the displacement amplitudes are symmetric with respect to the vertical axis, x = 0, when the P wave is incident vertically. The results indicates that considering the effect on the case with canyon on scattering of P wave, especially at high incident η, is requisite as researching ground motion.

4. Accuracy verification

4.1. Reduced verification (from pure theoretical point of view)

The distinction between the stratified media and the non-stratified media is that the physical parameters of two layers of media are different. We assume that Lame coefficients of two layers $\lambda_v = \lambda_s = \lambda$, $\mu_v = \mu_s = \mu$ and mass density $\rho_v = \rho_s = \rho$, respectively. Therefore, the solution of the stratified case would reduce to that of the non-stratified case.

So, the following equations can be obtained:

$$\alpha_v = \alpha_s = \sqrt{\frac{\lambda + 2\mu}{\rho}},\ \alpha_v = \alpha_s = \sqrt{\frac{\lambda + 2\mu}{\rho}} \tag{50}$$

$$k_{v\alpha} = \frac{\omega}{\alpha_v} = \frac{\omega}{\alpha_s} = k_{s\alpha},\ k_{v\beta} = \frac{\omega}{\beta_v} = \frac{\omega}{\beta_s} = k_{s\beta} \tag{51}$$

Based on Eqs. (50) and (51), the following expressions can respectively be given.

$$\begin{bmatrix} E_{11}^{v_o(1)}(n,R) & E_{12}^{v_o(1)+}(n,R) \\ E_{21}^{v_o(1)-}(n,R) & E_{22}^{v_o(1)}(n,R) \end{bmatrix} = \begin{bmatrix} E_{11}^{s_o(1)}(n,R) & E_{12}^{s_o(1)+}(n,R) \\ E_{21}^{s_o(1)-}(n,R) & E_{22}^{vs(1)}(n,R) \end{bmatrix} \tag{52a}$$

$$\begin{bmatrix} I_{11}^{v_o(1)}(n,R) & I_{12}^{v_o(1)+}(n,R) \\ I_{21}^{v_o(1)-}(n,R) & I_{22}^{v_o(1)}(n,R) \end{bmatrix} = \begin{bmatrix} I_{11}^{s_o(1)}(n,R) & I_{12}^{s_o(1)+}(n,R) \\ I_{21}^{s_o(1)-}(n,R) & I_{22}^{vs(1)}(n,R) \end{bmatrix} \tag{52b}$$

Combining Eq. (29)–(31) and (53) it yields

$$\frac{2\mu_v}{R^2}\sum_{n=0}^{\infty}\begin{bmatrix} E_{11}^{v_o(1)}(n,R) & E_{12}^{v_o(1)+}(n,R) \\ E_{21}^{v_o(1)-}(n,R) & E_{22}^{v_o(1)}(n,R)\end{bmatrix}\left(\begin{Bmatrix} A_{v1,n}^{(2)}+A_{v0,n}^{(2)}+A_{1,n} \\ C_{v1,n}^{(2)}+C_{v0,n}^{(2)}+C_{1,n}\end{Bmatrix}-\begin{Bmatrix} A_{s1,n}^{(2)}+A_{s2,n}^{(2)}+A_{s0,n}^{(2)}+A_{0,n} \\ C_{s1,n}^{(2)}+C_{s2,n}^{(2)}+C_{s0,n}^{(2)}+C_{0,n}\end{Bmatrix}\right)\left\langle\frac{\cos n\theta_2}{\sin n\theta_2}\right\rangle$$
$$+\frac{2\mu_v}{R^2}\sum_{n=0}^{\infty}\begin{bmatrix} E_{11}^{v_o(a)}(n,R) & E_{12}^{v_o(a)+}(n,R) \\ E_{21}^{v_o(a)-}(n,R) & E_{22}^{v_o(a)}(n,R)\end{bmatrix}\begin{Bmatrix} A_{v5,n}^{(2)} \\ C_{v5,n}^{(2)}\end{Bmatrix}\left\langle\frac{\cos n\theta_2}{\sin n\theta_2}\right\rangle$$
$$=\begin{Bmatrix}0\\0\end{Bmatrix}\frac{2\mu_v}{R^2}\sum_{n=0}^{\infty}\begin{bmatrix} E_{11}^{v_o(1)}(n,R) & E_{12}^{v_o(1)+}(n,R) \\ E_{21}^{v_o(1)-}(n,R) & E_{22}^{v_o(1)}(n,R)\end{bmatrix}\left(\begin{Bmatrix} B_{v1,n}^{(2)}+B_{v0,n}^{(2)}+B_{1,n} \\ D_{v1,n}^{(2)}+D_{v0,n}^{(2)}+D_{1,n}\end{Bmatrix}-\begin{Bmatrix} B_{s1,n}^{(2)}+B_{s2,n}^{(2)}+B_{s0,n}^{(2)}+B_{0,n} \\ D_{s1,n}^{(2)}+D_{s2,n}^{(2)}+D_{s0,n}^{(2)}+D_{0,n}\end{Bmatrix}\right)\left\langle\frac{\cos n\theta_2}{\sin n\theta_2}\right\rangle$$
$$+\frac{2\mu_v}{R^2}\sum_{n=0}^{\infty}\begin{bmatrix} E_{11}^{v_o(a)}(n,R) & E_{12}^{v_o(a)+}(n,R) \\ E_{21}^{v_o(a)-}(n,R) & E_{22}^{v_o(a)}(n,R)\end{bmatrix}\begin{Bmatrix} A_{v5,n}^{(2)} \\ C_{v5,n}^{(2)}\end{Bmatrix}\left\langle\frac{\cos n\theta_2}{\sin n\theta_2}\right\rangle=\begin{Bmatrix}0\\0\end{Bmatrix} \tag{53a}$$

$$\sum_{n=0}^{\infty}\begin{bmatrix} I_{11}^{v_o(1)}(n,R) & I_{12}^{v_o(1)+}(n,R) \\ I_{21}^{v_o(1)-}(n,R) & I_{22}^{v_o(1)}(n,R)\end{bmatrix}\left(\begin{Bmatrix} A_{v1,n}^{(2)}+A_{v0,n}^{(2)}+A_{1,n} \\ C_{v1,n}^{(2)}+C_{v0,n}^{(2)}+C_{1,n}\end{Bmatrix}-\begin{Bmatrix} A_{s1,n}^{(2)}+A_{s2,n}^{(2)}+A_{s0,n}^{(2)}+A_{0,n} \\ C_{s1,n}^{(2)}+C_{s2,n}^{(2)}+C_{s0,n}^{(2)}+C_{0,n}\end{Bmatrix}\right)\left\langle\frac{\cos n\theta_2}{\sin n\theta_2}\right\rangle$$
$$+\sum_{n=0}^{\infty}\begin{bmatrix} I_{11}^{v_o(a)}(n,R) & I_{12}^{v_o(a)+}(n,R) \\ I_{21}^{v_o(a)-}(n,R) & I_{22}^{v_o(a)}(n,R)\end{bmatrix}\begin{Bmatrix} A_{v5,n}^{(2)} \\ C_{v5,n}^{(2)}\end{Bmatrix}\left\langle\frac{\cos n\theta_2}{\sin n\theta_2}\right\rangle \tag{53b}$$
$$+\sum_{n=0}^{\infty}\begin{bmatrix} I_{11}^{v_o(1)}(n,R) & I_{12}^{v_o(1)+}(n,R) \\ I_{21}^{v_o(1)-}(n,R) & I_{22}^{v_o(1)}(n,R)\end{bmatrix}\left(\begin{Bmatrix} B_{v1,n}^{(2)}+B_{v0,n}^{(2)}+B_{1,n} \\ D_{v1,n}^{(2)}+D_{v0,n}^{(2)}+D_{1,n}\end{Bmatrix}-\begin{Bmatrix} B_{s1,n}^{(2)}+B_{s2,n}^{(2)}+B_{s0,n}^{(2)}+B_{0,n} \\ D_{s1,n}^{(2)}+D_{s2,n}^{(2)}+D_{s0,n}^{(2)}+D_{0,n}\end{Bmatrix}\right)\left\langle\frac{\sin n\theta_2}{\cos n\theta_2}\right\rangle$$
$$+\sum_{n=0}^{\infty}\begin{bmatrix} I_{11}^{v_o(a)}(n,R) & I_{12}^{v_o(a)+}(n,R) \\ I_{21}^{v_o(a)-}(n,R) & I_{22}^{v_o(a)}(n,R)\end{bmatrix}\begin{Bmatrix} B_{v5,n}^{(2)} \\ D_{v5,n}^{(2)}\end{Bmatrix}\left\langle\frac{\sin n\theta_2}{\cos n\theta_2}\right\rangle=\begin{Bmatrix}0\\0\end{Bmatrix}$$

Considering the orthogonality of the trigonometric functions, Eq. (53) result in

$$\begin{Bmatrix} A_{v1,n}^{(2)}+A_{v0,n}^{(2)}+A_{1,n} \\ C_{v1,n}^{(2)}+C_{v0,n}^{(2)}+C_{1,n}\end{Bmatrix}=\begin{Bmatrix} A_{s1,n}^{(2)}+A_{s2,n}^{(2)}+A_{s0,n}^{(2)}+A_{0,n} \\ C_{s1,n}^{(2)}+C_{s2,n}^{(2)}+C_{s0,n}^{(2)}+C_{0,n}\end{Bmatrix} \tag{54a}$$

$$\begin{Bmatrix} B_{v1,n}^{(2)}+B_{v0,n}^{(2)}+B_{1,n} \\ D_{v1,n}^{(2)}+D_{v0,n}^{(2)}+D_{1,n}\end{Bmatrix}=\begin{Bmatrix} B_{s1,n}^{(2)}+B_{s2,n}^{(2)}+B_{s0,n}^{(2)}+B_{0,n} \\ D_{s1,n}^{(2)}+D_{s2,n}^{(2)}+D_{s0,n}^{(2)}+D_{0,n}\end{Bmatrix} \tag{54b}$$

$$\begin{Bmatrix} A_{v5,n}^{(2)} \\ C_{v5,n}^{(2)}\end{Bmatrix}=\begin{Bmatrix}0\\0\end{Bmatrix} \tag{55a}$$

$$\begin{Bmatrix} B_{v5,n}^{(2)} \\ D_{v5,n}^{(2)}\end{Bmatrix}=\begin{Bmatrix}0\\0\end{Bmatrix} \tag{55b}$$

From Eq. (54), we have

$$\phi_v=\phi_s,\psi_v=\psi_s \tag{56}$$

It indicates that the wave functions in Layer-V and Layer-S are equal to each other, which fully satisfies the situation of the non-stratified case.

4.2. Verification (by numerical approach and comparison)

In order to verify the accuracy of the theoretical approach in this paper, the other is the method by numerical approach and comparing with classical example results, the aim of which is to further verify that whether the calculation results of with canyon are consistent with those of without canyon [40] while width and depth of the canyon are assumed to be zero ($h=2b=0$). It noted that the distinction between the canyon media and without canyon media is that whether width and depth of the canyon are zero. So, to compare with the accuracy of the solution above, we assume that width and depth of the canyon are zero. Therefore, the solution of the canyon case would reduce to that of without canyon case. The comparison diagram between this paper and Ref. [40] is showed in Fig. 10.

To obtain the numerical results using the method and our coded program, and further compared them with those in Ref. [40]; the material (λ, ρ, μ) and geometric materials need to be kept consistently. Here, the required material parameters are given below (see Table 1).

The x-displacements and y-displacements are calculated and compared with those of Ref. [40] for the case of dimensionless frequency $\eta = 1.0$ and $\eta = 4.0$ while incidence angle $i_d = 0$ in this paper. The comparison results are given in Fig. 11 and Fig. 12. It can be seen from the figures following that the calculation results are generally consistent with those of Ref. [40]. However, it can also be found that there exist the relative differences, especially while the value of x/a is in the range of [-0.5, 0.5] in Fig. 11(b), and in the range of [-1.5, −0.5] and [0.5, 1.5] in Fig. 12(a), respectively (see Table 1). The adoption of the large-arc method may be the reasons why to lead to the differences. As a result, it illustrates the precision of the proposed theoretical solution in this paper is satisfactory. The formulas used in Ref. [40] are listed in the following table (Table 2).

Where α, β represent the velocity of P and SV wave, respectively, p and η are $sin\ (i)/\alpha$ and $(1/(\alpha^2)\text{-}p^2)^{1/2}$.

5. Concluding remarks

(1) The theoretical solution is derived and verified for scattering problem of P waves incidence on V-shaped canyon of the second stratification type (type II). The challenge to conduct the study is that to deal with the boundary conditions in vertical direction on canyon surface and layer-interface crossing canyon of type II, which logically leads to more coordinate system transformations and more complex solution process due to the unknown

coefficients need to be converted between the more different coordinates. Moreover, the ground motion displacement is discussed base on the derived theoretical solution, and the influence of the effect of layered canyon of type II on scattering is discussed as well for different frequencies and incident angles.

(2) The influence of the scattering of P waves on the ground motion is compared between the non-layered and double-layered model in here. The results demonstrate that the double-layer effect have significant influence on both the x- and y-component displacements amplitudes of ground surface, and it causes relatively greater vibration for surface displacement comparing with non-layered model. In addition, considering the influence of the frequencies of incident waves on the amplitudes of surface displacements, the surface displacements present larger amplitudes and fluctuations relatively with the increase of incident wave frequencies. Finally, the effect of incident angles on ground motion displacement is also studied, incident angles have a remarkable influence on the amplitudes of surface displacements: amplitudes and fluctuations of surface displacements increase with an increasing incident angle. Moreover, it is obvious that both the *x*- and *y*-component displacement amplitudes are more significantly magnified when the incident waves with high frequencies at large incident angles. Therefore, it is inadequate that non-layered canyon replaces double-layered model for simulating earthquake and seismic assessment. The factor of frequencies and incident angles should be fully considered.

(3) By comparing the both the *x*- and *y*-component displacement amplitudes with and without canyon, it is concluded that, for this type of canyon, the remarkable influence on the scattering of high frequencies incident is found, which can obviously amplify not only amplitudes but also fluctuations of surface displacements. So, the ideal assumption of uniform medium and (or) the first stratification type (not crossing canyon by layer-interface only for solution convenience) is suggested should be adopted carefully.

Author contributions statement

Liu Guohuan(corresponding author):Conceptualization, Methodology, Writing-Reviewing and Editing, Investigation, Resources, Fund support.

Feng Guangrui : Writing-Original draft preparation, Data curation, Software, Review and Editing, Proofread Grammar.

Declaration of competing interest

The authors declare that they have no known competing financial interests or personal relationships that could have appeared to influence the work reported in this paper.

Acknowledgement

The authors acknowledge the support from the National Natural Science Foundation of China (Grant No.51978461 and 51778414), and the State Key Lab of Subtropical Building Science, South China University of Technology (Grant No.2017ZB21).

APPENDIX-A. reflection and transmittance coefficients

$$\begin{cases} k_{p1v} = \dfrac{\sin 2t_d \cos 2i_{vp} - (\alpha_v/\beta_v)^2 \cos^2 2i_{vp}}{\sin 2t_d \cos 2i_{vp} + (\alpha_v/\beta_v)^2 \cos^2 2i_{vp}} \\ k_{p2v} = \dfrac{-2 \sin 2t_d \cos 2i_{vp}}{\sin 2t_d \cos 2i_{vp} + (\alpha_v/\beta_v)^2 \cos^2 2i_{vp}} \end{cases} \tag{A1}$$

$$\begin{cases} k_{s1v} = \dfrac{2(\alpha_v/\beta_v)^2 \sin 2t_s \cos 2t_s}{\sin 2i_{vs} \sin 2t_s + (\alpha_v/\beta_v)^2 \cos^2 2t_s} \\ k_{s2v} = \dfrac{\sin 2i_{vs} \sin 2t_s - (\alpha_v/\beta_v)^2 \cos^2 2t_s}{\sin 2i_{vs} \sin 2t_s + (\alpha_v/\beta_v)^2 \cos^2 2t_s} \end{cases} \tag{A2}$$

$$\begin{Bmatrix} A_{0,m} \\ B_{0,m} \end{Bmatrix} = \varepsilon_m i^m \begin{Bmatrix} \cos mi_d \\ \sin mi_d \end{Bmatrix} [\pm (-1)^m \exp(-id_2 k_{s\alpha} \cos i_d) + k_{s1} \exp(id_2 k_{s\alpha} \cos i_d)] \tag{A3}$$

$$\begin{Bmatrix} C_{0,m} \\ D_{0,m} \end{Bmatrix} = \varepsilon_m i^m \begin{Bmatrix} \sin mi_s \\ \cos mi_s \end{Bmatrix} [k_{s2} \exp(id_2 k_{s\beta} \cos i_s)] \tag{A4}$$

$$\begin{aligned} \begin{Bmatrix} A_{1,m} \\ B_{1,m} \end{Bmatrix} &= \varepsilon_m i^m \begin{Bmatrix} \cos mt_d \\ \sin mt_d \end{Bmatrix} \left[\pm (-1)^m t_1 \exp - id_2 k_{v\alpha} \cos t_d + k_{p1v} t_1 \exp(id_2 k_{v\alpha} \cos t_d) \right] \\ &+ \varepsilon_m i^m \begin{Bmatrix} \cos mi_{vs} \\ \sin mi_{vs} \end{Bmatrix} [k_{s1v} t_2 \exp(id_2 k_{v\alpha} \cos i_{vs})] \end{aligned} \tag{A5}$$

$$\begin{aligned} \begin{Bmatrix} C_{1,m} \\ D_{1,m} \end{Bmatrix} &= \varepsilon_m i^m \begin{Bmatrix} \sin mt_s \\ \cos mt_s \end{Bmatrix} [\mp (-1)^m t_2 \exp - id_2 k_{v\beta} \cos t_s + k_{s2v} t_2 \exp(id_2 k_{v\beta} \cos t_s)] \\ &+ \varepsilon_m i^m \begin{Bmatrix} \sin mi_{vp} \\ \cos mi_{vp} \end{Bmatrix} \left[k_{p2v} t_1 \exp\left(id_2 k_{v\beta} \cos i_{vp} \right) \right] \end{aligned} \tag{A6}$$

where ε_m is Neumann factor and $(\varepsilon_0 = 1; \varepsilon_m = 2, m \geq 1)$, and same as that in the following.

APPENDIX-B. expression solutions of scattering waves as Fourier-Bessel series

$$\varphi_{s1}\left(r_2,\theta_2\right)=\sum_{n=0}^{\infty}J_n\left(k_{s\alpha}r_2\right)\left(A_{s1,n}^{(2)}\cos n\theta_2+B_{s1,n}^{(2)}\sin n\theta_2\right)\ ;\ \psi_{s1}\left(r_2,\theta_2\right)=\sum_{n=0}^{\infty}J_n\left(k_{s\beta}r_2\right)\left(C_{s1,n}^{(2)}\cos n\theta_2+D_{s1,n}^{(2)}\sin n\theta_2\right) \tag{B1}$$

$$\varphi_{s2}\left(r_1,\theta_1\right)=\sum_{M=0}^{\infty}H_m^{(1)}\left(k_{s\alpha}r_1\right)\left(A_{s2,m}^{(1)}\cos m\theta_1+B_{s2,m}^{(1)}\sin m\theta_1\right)\ ;\ \psi_{s2}\left(r_1,\theta_1\right)=\sum_{m=0}^{\infty}H_m^{(1)}\left(k_{s\beta}r_1\right)\left(C_{s2,m}^{(1)}\cos m\theta_1+D_{s2,m}^{(1)}\sin m\theta_1\right) \tag{B2}$$

$$\varphi_{s0}\left(r_1,\theta_1\right)=\sum_{m=0}^{\infty}H_m^{(1)}\left(k_{s\alpha}r_1\right)\left(A_{s0,m}^{(1)}\cos m\theta_1+B_{s0,m}^{(1)}\sin m\theta_1\right)\ ;\psi_{s0}\left(r_1,\theta_1\right)=\sum_{n=0}^{\infty}H_m^{(1)}\left(k_{s\beta}r_1\right)\left(C_{s0,m}^{(1)}\sin m\theta_1+D_{s0,m}^{(1)}\cos m\theta_1\right) \tag{B3}$$

$$\varphi_{v1}\left(r_2,\theta_2\right)=\sum_{n=0}^{\infty}J_n\left(k_{v\alpha}r_2\right)\left(A_{v1,n}^{(2)}\cos n\theta_2+B_{v1,n}^{(2)}\sin n\theta_2\right)\ ;\psi_{v1}\left(r_2,\theta_2\right)=\sum_{n=0}^{\infty}J_n\left(k_{v\beta}r_2\right)\left(C_{v1,n}^{(2)}\cos n\theta_2+D_{v1,n}^{(2)}\sin n\theta_2\right) \tag{B4}$$

$$\varphi_{v2}\left(r_1,\theta_1\right)=\sum_{m=0}^{\infty}H_m^{(1)}\left(k_{v\alpha}r_1\right)\left(A_{v2,m}^{(1)}\cos m\theta_1+B_{v2,m}^{(1)}\sin m\theta_1\right)\ ;\psi_{v2}\left(r_1,\theta_1\right)=\sum_{n=0}^{\infty}H_m^{(1)}\left(k_{v\beta}r_1\right)\left(C_{v2,m}^{(1)}\sin m\theta_1+D_{v2,m}^{(1)}\cos m\theta_1\right) \tag{B5}$$

$$\varphi_{v0}\left(r_1,\theta_1\right)=\sum_{m=0}^{\infty}H_m^{(1)}\left(k_{v\alpha}r_1\right)\left(A_{v0,m}^{(1)}\cos m\theta_1+B_{v0,m}^{(1)}\sin m\theta_1\right)\ ;\psi_{v0}\left(r_1,\theta_1\right)=\sum_{n=0}^{\infty}H_m^{(1)}\left(k_{v\beta}r_1\right)\left(C_{v0,m}^{(1)}\sin m\theta_1+D_{v0,m}^{(1)}\cos m\theta_1\right) \tag{B6}$$

$$\varphi_{v5}\left(r_2,\theta_2\right)=\sum_{n=0}^{\infty}H_n^{(1)}\left(k_{v\alpha}r_2\right)\left(A_{v5,n}^{(2)}\cos n\theta_2+B_{v5,n}^{(2)}\sin n\theta_2\right)\ ;\psi_{v5}\left(r_2,\theta_2\right)=\sum_{n=0}^{\infty}H_n^{(1)}\left(k_{v\beta}r_2\right)\left(C_{v5,n}^{(2)}\sin n\theta_2+D_{v5,n}^{(2)}\cos n\theta_2\right) \tag{B7}$$

$$\varphi_{s4}^{L}\left(r_3,\theta_3\right)=\sum_{l=0}^{\infty}H_l^{(1)}\left(k_{s\alpha}r_3\right)\left(A_{s4,l}^{(3)}\cos l\theta_3+B_{s4,l}^{(3)}\sin l\theta_3\right)\ ;\psi_{s4}^{L}\left(r_3,\theta_3\right)=\sum_{l=0}^{\infty}H_l^{(1)}\left(k_{s\beta}r_3\right)\left(C_{s4,l}^{(3)}\sin l\theta_3+D_{s4,l}^{(3)}\cos l\theta_3\right) \tag{B8}$$

$$\varphi_{s4}^{R}\left(r_4,\theta_4\right)=\sum_{r=0}^{\infty}H_r^{(1)}\left(k_{s\alpha}r_4\right)\left(A_{s4,r}^{(4)}\cos r\theta_4+B_{s4,r}^{(4)}\sin r\theta_4\right)\ ;\ \psi_{s4}^{R}\left(r_4,\theta_4\right)=\sum_{r=0}^{\infty}H_r^{(1)}\left(k_{s\beta}r_4\right)\left(C_{s4,r}^{(4)}\sin r\theta_4+D_{s4,r}^{(4)}\cos r\theta_4\right) \tag{B9}$$

$$\varphi_{v4}^{L}\left(r_3,\theta_3\right)=\sum_{l=0}^{\infty}H_l^{(1)}\left(k_{v\alpha}r_3\right)\left(A_{v4,l}^{(3)}\cos l\theta_3+B_{v4,l}^{(3)}\sin l\theta_3\right)\ ;\psi_{v4}^{L}\left(r_3,\theta_3\right)=\sum_{l=0}^{\infty}H_l^{(1)}\left(k_{v\beta}r_3\right)\left(C_{v4,l}^{(3)}\sin l\theta_4+D_{v4,l}^{(3)}\cos l\theta_4\right) \tag{B10}$$

$$\varphi_{v4}^{R}\left(r_4,\theta_4\right)=\sum_{r=0}^{\infty}H_r^{(1)}\left(k_{v\alpha}r_4\right)\left(A_{v4,r}^{(4)}\cos r\theta_4+B_{v4,r}^{(4)}\sin r\theta_4\right)\ ;\psi_{v4}^{R}\left(r_4,\theta_4\right)=\sum_{r=0}^{\infty}H_r^{(1)}\left(k_{v\beta}r_4\right)\left(C_{v4,r}^{(4)}\sin r\theta_4+D_{v4,r}^{(4)}\cos r\theta_4\right) \tag{B11}$$

$$\varphi_{s6}\left(r_2,\theta_2\right)=\sum_{n=0}^{\infty}J_n\left(k_{s\alpha}r_2\right)\left(A_{s6,n}^{(2)}\cos n\theta_2+B_{s6,n}^{(2)}\sin n\theta_2\right)\ ;\ \psi_{s6}\left(r_2,\theta_2\right)=\sum_{n=0}^{\infty}J_n\left(k_{s\beta}r_2\right)\left(C_{s6,n}^{(2)}\cos n\theta_2+D_{s6,n}^{(2)}\sin n\theta_2\right) \tag{B12}$$

$$\varphi_{v7}\left(r_2,\theta_2\right)=\sum_{n=0}^{\infty}H_n^{(1)}\left(k_{v\alpha}r_2\right)\left(A_{v7,n}^{(2)}\cos n\theta_2+B_{v7,n}^{(2)}\sin n\theta_2\right)\ ;\psi_{v7}\left(r_2,\theta_2\right)=\sum_{n=0}^{\infty}H_n^{(1)}\left(k_{v\beta}r_2\right)\left(C_{v7,n}^{(2)}\sin n\theta_2+D_{v7,n}^{(2)}\cos n\theta_2\right) \tag{B13}$$

where $H_m^{(1)}(*)$ is the Hankel function, and $A_{s1,n}^{(2)}\sim D_{v7,n}^{(2)}$ are a series of unknown coefficient.

APPENDIX-C. The coordinate transformation

Transformation between $r_1-\theta_1$ and $r_2-\theta_2$:

$$\varphi^{(i+r)}(r_2,\theta_2)=\sum_{n=0}^{\infty}J_n(k_{s\alpha}r_2)\left(A_{0,n}\cos n\theta_2+B_{0,n}\sin n\theta_2\right)\qquad\begin{Bmatrix}A_{0,n}\\B_{0,n}\end{Bmatrix}=\sum_{m=0}^{\infty}F1_{nm}^{\pm}(k_{s\alpha}D_{12})\begin{Bmatrix}A_{0,m}\\B_{0,m}\end{Bmatrix} \tag{C1}$$

$$\varphi^{(r)}(r_2,\theta_2)=\sum_{n=0}^{\infty}J_n(k_{s\beta}r_2)\left(C_{0,n}\sin n\theta_2+D_{0,n}\cos n\theta_2\right)\qquad\begin{Bmatrix}C_{0,n}\\D_{0,n}\end{Bmatrix}=\sum_{m=0}^{\infty}F1_{nm}^{\pm}(k_{s\beta}D_{12})\begin{Bmatrix}C_{0,m}\\D_{0,m}\end{Bmatrix} \tag{C2}$$

$$\varphi^{(t+r)}(r_2,\theta_2)=\sum_{n=0}^{\infty}J_n(k_{v\alpha}r_2)\left(A_{1,n}\cos n\theta_2+B_{1,n}\sin n\theta_2\right)\qquad\begin{Bmatrix}A_{1,n}\\B_{1,n}\end{Bmatrix}=\sum_{n=0}^{\infty}F1_{nm}^{\pm}(k_{v\alpha}D_{12})\begin{Bmatrix}A_{1,m}\\B_{1,m}\end{Bmatrix} \tag{C3}$$

$$\varphi^{(t+r)}(r_2,\theta_2)=\sum_{n=0}^{\infty}J_n(k_{v\beta}r_2)\left(C_{1,n}\sin n\theta_2+D_{1,n}\cos n\theta_2\right)\qquad\begin{Bmatrix}C_{1,n}\\D_{1,n}\end{Bmatrix}=\sum_{n=0}^{\infty}F1_{nm}^{\pm}(k_{v\beta}D_{12})\begin{Bmatrix}C_{1,m}\\D_{1,m}\end{Bmatrix} \tag{C4}$$

$$\varphi_{s1}(r_1,\theta_1)=\sum_{m=0}^{\infty}J_m(k_{s\alpha}r_1)\left(A_{s1,m}^{(1)}\cos m\theta_1+B_{s1,m}^{(1)}\sin m\theta_1\right)\qquad\begin{Bmatrix}A_{s1,m}^{(1)}\\B_{s1,m}^{(1)}\end{Bmatrix}=\sum_{n=0}^{\infty}F1_{nm}^{\pm}(k_{s\alpha}D_{12})\begin{Bmatrix}A_{s1,n}^{(2)}\\B_{s1,n}^{(2)}\end{Bmatrix} \tag{C5}$$

$$\psi_{s1}(r_1,\theta_1)=\sum_{m=0}^{\infty}J_m(k_{s\beta}r_1)\left(C_{s1,m}^{(1)}\sin m\theta_1+D_{s1,m}^{(1)}\cos m\theta_1\right)\quad\begin{Bmatrix}C_{s1,m}^{(1)}\\D_{s1,m}^{(1)}\end{Bmatrix}=\sum_{n=0}^{\infty}F1_{nm}^{\pm}(k_{s\beta}D_{12})\begin{Bmatrix}C_{s1,n}^{(2)}\\D_{s1,n}^{(2)}\end{Bmatrix}\tag{C6}$$

$$\varphi_{s2}(r_2,\theta_2)=\sum_{n=0}^{\infty}J_n(k_{s\alpha}r_2)\left(A_{s2,n}^{(2)}\cos n\theta_2+B_{s2,n}^{(2)}\sin n\theta_2\right)\quad\begin{Bmatrix}A_{s2,n}^{(2)}\\B_{s2,n}^{(2)}\end{Bmatrix}=\sum_{m=0}^{\infty}F2_{nm}^{\pm}(k_{s\alpha}D_{12})\begin{Bmatrix}A_{s2,m}^{(1)}\\B_{s2,m}^{(1)}\end{Bmatrix}\tag{C7}$$

$$\psi_{s2}(r_2,\theta_2)=\sum_{n=0}^{\infty}J_n(k_{s\beta}r_2)\left(C_{s2,n}^{(2)}\sin n\theta_2+D_{s2,n}^{(2)}\cos n\theta_2\right)\quad\begin{Bmatrix}C_{s2,n}^{(2)}\\D_{s2,n}^{(2)}\end{Bmatrix}=\sum_{m=0}^{\infty}F2_{nm}^{\pm}(k_{s\beta}D_{12})\begin{Bmatrix}C_{s2,m}^{(1)}\\D_{s2,m}^{(1)}\end{Bmatrix}\tag{C8}$$

$$\varphi_{s0}(r_2,\theta_2)=\sum_{n=0}^{\infty}J_n(k_{s\alpha}r_2)\left(A_{s0,n}^{(2)}\cos n\theta_2+B_{s0,n}^{(2)}\sin n\theta_2\right)\quad\begin{Bmatrix}A_{s0,n}^{(2)}\\B_{s0,n}^{(2)}\end{Bmatrix}=\sum_{m=0}^{\infty}F2_{nm}^{\pm}(k_{s\alpha}D_{12})\begin{Bmatrix}A_{s0,m}^{(1)}\\B_{s0,m}^{(1)}\end{Bmatrix}\tag{C9}$$

$$\psi_{s0}(r_2,\theta_2)=\sum_{n=0}^{\infty}J_n(k_{s\beta}r_2)\left(C_{s0,n}^{(2)}\sin n\theta_2+D_{s0,n}^{(2)}\cos n\theta_2\right)\quad\begin{Bmatrix}C_{s0,n}^{(2)}\\D_{s0,n}^{(2)}\end{Bmatrix}=\sum_{m=0}^{\infty}F2_{nm}^{\pm}(k_{s\beta}D_{12})\begin{Bmatrix}C_{s0,m}^{(1)}\\D_{s0,m}^{(1)}\end{Bmatrix}\tag{C10}$$

$$\varphi_{v1}(r_1,\theta_1)=\sum_{m=0}^{\infty}J_m(k_{v\alpha}r_1)\left(A_{v1,m}^{(1)}\cos m\theta_1+B_{v1,m}^{(1)}\sin m\theta_1\right)\quad\begin{Bmatrix}A_{v1,m}^{(1)}\\B_{v1,m}^{(1)}\end{Bmatrix}=\sum_{n=0}^{\infty}F1_{nm}^{\pm}(k_{v\alpha}D_{12})\begin{Bmatrix}A_{v1,n}^{(2)}\\B_{v1,n}^{(2)}\end{Bmatrix}\tag{C11}$$

$$\psi_{v1}(r_1,\theta_1)=\sum_{m=0}^{\infty}J_m(k_{v\beta}r_1)\left(C_{v1,m}^{(1)}\sin m\theta_1+D_{v1,m}^{(1)}\cos m\theta_1\right)\quad\begin{Bmatrix}C_{v1,m}^{(1)}\\D_{v1,m}^{(1)}\end{Bmatrix}=\sum_{n=0}^{\infty}F1_{nm}^{\pm}(k_{v\beta}D_{12})\begin{Bmatrix}C_{v1,n}^{(2)}\\D_{v1,n}^{(2)}\end{Bmatrix}\tag{C12}$$

$$\varphi_{v2}(r_2,\theta_2)=\sum_{n=0}^{\infty}J_n(k_{v\alpha}r_2)\left(A_{v2,n}^{(2)}\cos m\theta_2+B_{v2,n}^{(2)}\sin m\theta_2\right)\quad\begin{Bmatrix}A_{v2,n}^{(2)}\\B_{v2,n}^{(2)}\end{Bmatrix}=\sum_{m=0}^{\infty}F2_{nm}^{\pm}(k_{v\alpha}D_{12})\begin{Bmatrix}A_{v2,m}^{(1)}\\B_{v2,m}^{(1)}\end{Bmatrix}\tag{C13}$$

$$\psi_{v2}(r_2,\theta_2)=\sum_{n=0}^{\infty}J_n(k_{v\beta}r_2)\left(C_{v2,n}^{(2)}\sin n\theta_2+D_{v2,n}^{(2)}\cos n\theta_2\right)\quad\begin{Bmatrix}C_{v2,n}^{(2)}\\D_{v2,n}^{(2)}\end{Bmatrix}=\sum_{m=0}^{\infty}F2_{nm}^{\pm}(k_{v\beta}D_{12})\begin{Bmatrix}C_{v2,m}^{(1)}\\D_{v2,m}^{(1)}\end{Bmatrix}\tag{C14}$$

$$\varphi_{v0}(r_2,\theta_2)=\sum_{n=0}^{\infty}J_n(k_{v\alpha}r_2)\left(A_{v0,n}^{(2)}\cos n\theta_2+B_{v0,n}^{(2)}\sin n\theta_2\right)\quad\begin{Bmatrix}A_{v0,n}^{(2)}\\B_{v0,n}^{(2)}\end{Bmatrix}=\sum_{m=0}^{\infty}F2_{nm}^{\pm}(k_{v\alpha}D_{12})\begin{Bmatrix}A_{v0,m}^{(1)}\\B_{v0,m}^{(1)}\end{Bmatrix}\tag{C15}$$

$$\psi_{v0}(r_2,\theta_2)=\sum_{n=0}^{\infty}J_n(k_{v\beta}r_2)\left(C_{v0,n}^{(2)}\sin n\theta_2+D_{v0,n}^{(2)}\cos n\theta_2\right)\quad\begin{Bmatrix}C_{v0,n}^{(2)}\\D_{v0,n}^{(2)}\end{Bmatrix}=\sum_{m=0}^{\infty}F2_{nm}^{\pm}(k_{v\beta}D_{12})\begin{Bmatrix}C_{v0,m}^{(1)}\\D_{v0,m}^{(1)}\end{Bmatrix}\tag{C16}$$

$$\psi_{v5}(r_1,\theta_1)=\sum_{m=0}^{\infty}J_{\mathrm{m}}(k_{v\alpha}r_1)(A_{v5,m}^{(1)}\cos n\theta_1+B_{v5,m}^{(1)}\cos m\theta_1)\{\begin{matrix}A_{v5,m}^{(1)}\\D_{v5,m}^{(1)}\end{matrix}\}=\sum_{n=0}^{\infty}F2_{nm}^{\pm}(k_{v\alpha}D_{12})\{\begin{matrix}A_{v5,n}^{(2)}\\D_{v5,n}^{(2)}\end{matrix}\}\tag{c17}$$

$$\psi_{v5}(r_1,\theta_1)=\sum_{m=0}^{\infty}J_m(k_{v\beta}r_1)\left(C_{v5,m}^{(1)}\sin m\theta_1+D_{v5,m}^{(1)}\cos m\theta_1\right)\begin{Bmatrix}C_{v5,m}^{(1)}\\D_{v5,m}^{(1)}\end{Bmatrix}=\sum_{n=0}^{\infty}F2_{nm}^{\pm}(k_{v\beta}D_{12})\begin{Bmatrix}C_{v5,n}^{(2)}\\D_{v5,n}^{(2)}\end{Bmatrix}\tag{C18}$$

where D_{12} is the distance between O_1 and O_2

$$\begin{cases}F1_{ij}^{\pm}(kD_{12})=\dfrac{1}{2}\varepsilon_i\left[J_{i+j}(kD_{12})\pm(-1)^jJ_{i-j}(kD_{12})\right]\\[2ex]F2_{ij}^{\pm}(kD_{12})=\dfrac{1}{2}\varepsilon_i\left[H_{i+j}^{(1)}(kD_{12})\pm(-1)^jH_{i+j}^{(1)}(kD_{12})\right]\end{cases}$$

Transformation from $r_3-\theta_3$ or $r_4-\theta_4$ to $r_1-\theta_1$ *or* $r_2-\theta_2$:

$$\Phi_{s4}^{L}(r_1,\theta_1)=\sum_{m=0}^{\infty}J_m(k_{s\alpha}r_1)\left(A_{s4,m}^{(1L)}\cos m\theta_1+B_{s4,m}^{(1L)}\sin m\theta_1\right)\begin{Bmatrix}A_{s4,m}^{(1L)}\\B_{s4,m}^{(1L)}\end{Bmatrix}=\sum_{l=0}^{\infty}\begin{bmatrix}T_{1,S}^{4L(3)}&T_{3,S}^{4L(3)}\\T_{2,S}^{4L(3)}&T_{4,S}^{4L(3)}\end{bmatrix}\begin{Bmatrix}A_{s4,l}^{(1L)}\\B_{s4,l}^{(1L)}\end{Bmatrix}\tag{c19}$$

$$\Psi_{s4}^{L}(r_1,\theta_1)=\sum_{m=0}^{\infty}J_m(k_{s\beta}r_1)\left(C_{s4,m}^{(1L)}\sin m\theta_1+D_{s4,m}^{(1L)}\cos m\theta_1\right)\begin{Bmatrix}C_{s4,m}^{(1L)}\\D_{s4,m}^{(1L)}\end{Bmatrix}=\sum_{l=0}^{\infty}\begin{bmatrix}T_{4,S}^{4L(3)}&T_{2,S}^{4L(3)}\\T_{3,S}^{4L(3)}&T_{1,S}^{4L(3)}\end{bmatrix}\begin{Bmatrix}C_{s4,l}^{(1L)}\\D_{s4,l}^{(1L)}\end{Bmatrix}\tag{c20}$$

$$\Phi_{s4}^{R}(r_1,\theta_1)=\sum_{m=0}^{\infty}J_m(k_{s\alpha}r_1)\left(A_{s4,m}^{(1R)}\cos m\theta_1+B_{s4,m}^{(1R)}\sin m\theta_1\right)\begin{Bmatrix}A_{s4,m}^{(1R)}\\B_{s4,m}^{(1R)}\end{Bmatrix}=\sum_{r=0}^{\infty}\begin{bmatrix}T_{1,S}^{4R(3)} & T_{3,S}^{4R(3)}\\T_{2,S}^{4R(3)} & T_{4,S}^{4R(3)}\end{bmatrix}\begin{Bmatrix}A_{s4,l}^{(1R)}\\B_{s4,l}^{(1R)}\end{Bmatrix} \tag{c21}$$

$$\Psi_{s4}^{R}(r_1,\theta_1)=\sum_{m=0}^{\infty}J_m(k_{s\beta}r_1)\left(C_{s4,m}^{(1R)}\sin m\theta_1+D_{s4,m}^{(1R)}\cos m\theta_1\right)\begin{Bmatrix}C_{s4,m}^{(1R)}\\D_{s4,m}^{(1R)}\end{Bmatrix}=\sum_{r=0}^{\infty}\begin{bmatrix}T_{4,S}^{4R(3)} & T_{2,S}^{4R(3)}\\T_{3,S}^{4R(3)} & T_{1,S}^{4R(3)}\end{bmatrix}\begin{Bmatrix}C_{s4,r}^{(1R)}\\D_{s4,r}^{(1R)}\end{Bmatrix} \tag{c22}$$

$$\Phi_{v4}^{L}(r_1,\theta_1)=\sum_{m=0}^{\infty}J_m(k_{v\alpha}r_1)\left(A_{v4,m}^{(1L)}\cos m\theta_1+B_{v4,m}^{(1L)}\sin m\theta_1\right)\begin{Bmatrix}A_{v4,m}^{(1L)}\\B_{v4,m}^{(1L)}\end{Bmatrix}=\sum_{l=0}^{\infty}\begin{bmatrix}T_{1,V}^{4L(3)} & T_{3,V}^{4L(3)}\\T_{2,V}^{4L(3)} & T_{4,V}^{4L(3)}\end{bmatrix}\begin{Bmatrix}A_{v4,l}^{(1L)}\\B_{v4,l}^{(1L)}\end{Bmatrix} \tag{c23}$$

$$\Psi_{v4}^{L}(r_1,\theta_1)=\sum_{m=0}^{\infty}J_m(k_{v\beta}r_1)\left(C_{v4,m}^{(1L)}\sin m\theta_1+D_{v4,m}^{(1L)}\cos m\theta_1\right)\begin{Bmatrix}C_{v4,m}^{(1L)}\\D_{v4,m}^{(1L)}\end{Bmatrix}=\sum_{l=0}^{\infty}\begin{bmatrix}T_{4,S}^{4R(3)} & T_{2,S}^{4R(3)}\\T_{3,S}^{4R(3)} & T_{1,S}^{4R(3)}\end{bmatrix}\begin{Bmatrix}C_{v4,l}^{(3)}\\D_{v4,l}^{(3)}\end{Bmatrix} \tag{c24}$$

$$\Phi_{v4}^{R}(r_1,\theta_1)=\sum_{m=0}^{\infty}J_m(k_{v\alpha}r_1)\left(A_{v4,m}^{(1R)}\cos m\theta_1+B_{v4,m}^{(1R)}\sin m\theta_1\right)\begin{Bmatrix}A_{v4,m}^{(1R)}\\B_{v4,m}^{(1R)}\end{Bmatrix}=\sum_{r=0}^{\infty}\begin{bmatrix}T_{1,V}^{4R(3)} & T_{3,V}^{4R(3)}\\T_{2,V}^{4R(3)} & T_{4,V}^{4R(3)}\end{bmatrix}\begin{Bmatrix}A_{v4,r}^{(1R)}\\B_{v4,r}^{(1R)}\end{Bmatrix} \tag{c25}$$

$$\Psi_{v4}^{R}(r_1,\theta_1)=\sum_{m=0}^{\infty}J_m(k_{v\beta}r_1)\left(C_{v4,m}^{(1R)}\sin m\theta_1+D_{v4,m}^{(1R)}\cos m\theta_1\right)\begin{Bmatrix}C_{v4,m}^{(1R)}\\D_{v4,m}^{(1R)}\end{Bmatrix}=\sum_{r=0}^{\infty}\begin{bmatrix}T_{4,V}^{4R(3)} & T_{2,V}^{4R(3)}\\T_{3,V}^{4R(3)} & T_{1,V}^{4R(3)}\end{bmatrix}\begin{Bmatrix}C_{v4,r}^{(3)}\\D_{v4,r}^{(3)}\end{Bmatrix} \tag{c26}$$

Where

$$\begin{cases}T_{1,*}^{3L(1)}=\cos l\alpha R1C_{ml}^{+}(k_*D_{13}\gamma_{13})+\sin l\alpha R2C_{ml}^{-}(k_*D_{13}\gamma_{13})\\T_{2,*}^{3L(1)}=\cos l\alpha R2C_{ml}^{+}(k_*D_{13}\gamma_{13})+\sin l\alpha R1C_{ml}^{-}(k_*D_{13}\gamma_{13})\\T_{3,*}^{3L(1)}=-\sin l\alpha R1C_{ml}^{+}(k_*D_{13}\gamma_{13})+\cos l\alpha R2C_{ml}^{-}(k_*D_{13}\gamma_{13})\\T_{4,*}^{3L(1)}=-\sin l\alpha R2C_{ml}^{+}(k_*D_{13}\gamma_{13})+\cos l\alpha R1C_{ml}^{-}(k_*D_{13}\gamma_{13})\end{cases}$$

$$\begin{cases}T_{1,*}^{3R(1)}=\cos r\alpha R1C_{mr}^{+}(k_*D_{13}\gamma_{13})+\sin r\alpha R2C_{mr}^{-}(k_*D_{13}\gamma_{13})\\T_{2,*}^{3R(1)}=\cos r\alpha R2C_{mr}^{+}(k_*D_{13}\gamma_{13})+\sin r\alpha R1C_{mr}^{-}(k_*D_{13}\gamma_{13})\\T_{3,*}^{3R(1)}=-\sin r\alpha R1C_{mr}^{+}(k_*D_{13}\gamma_{13})+\cos r\alpha R2C_{mr}^{-}(k_*D_{13}\gamma_{13})\\T_{4,*}^{3R(1)}=-\sin r\alpha R2C_{mr}^{+}(k_*D_{13}\gamma_{13})+\cos r\alpha R1C_{mr}^{-}(k_*D_{13}\gamma_{13})\end{cases}$$

$$\begin{cases}T_{1,*}^{4L(1)}=\cos l\alpha R1C_{ml}^{+}(k_*D_{14}\gamma_{14})+\sin l\alpha R2C_{ml}^{-}(k_*D_{14}\gamma_{14})\\T_{2,*}^{4L(1)}=\cos l\alpha R2C_{ml}^{+}(k_*D_{14}\gamma_{14})+\sin l\alpha R1C_{ml}^{-}(k_*D_{14}\gamma_{14})\\T_{3,*}^{4L(1)}=-\sin l\alpha R1C_{ml}^{+}(k_*D_{14}\gamma_{14})+\cos l\alpha R2C_{ml}^{-}(k_*D_{14}\gamma_{14})\\T_{4,*}^{4L(1)}=-\sin l\alpha R2C_{ml}^{+}(k_*D_{14}\gamma_{14})+\cos l\alpha R1C_{ml}^{-}(k_*D_{14}\gamma_{14})\end{cases}$$

$$\begin{cases}T_{1,*}^{4L(1)}=\cos l\alpha R1C_{ml}^{+}(k_*D_{14}\gamma_{14})+\sin l\alpha R2C_{ml}^{-}(k_*D_{14}\gamma_{14})\\T_{2,*}^{4L(1)}=\cos l\alpha R2C_{ml}^{+}(k_*D_{14}\gamma_{14})+\sin l\alpha R1C_{ml}^{-}(k_*D_{14}\gamma_{14})\\T_{3,*}^{4L(1)}=-\sin l\alpha R1C_{ml}^{+}(k_*D_{14}\gamma_{14})+\cos l\alpha R2C_{ml}^{-}(k_*D_{14}\gamma_{14})\\T_{4,*}^{4L(1)}=-\sin l\alpha R2C_{ml}^{+}(k_*D_{14}\gamma_{14})+\cos l\alpha R1C_{ml}^{-}(k_*D_{14}\gamma_{14})\end{cases}$$

where

$$\begin{cases}R1C_{mn}^{\pm}(e\gamma)=\dfrac{\varepsilon_m}{2}[\pm C_{m+n}(e)\cos(m+n)\gamma+(-1)^nC_{m-n}(e)\cos(m-n)\gamma]\\R2C_{mn}^{\pm}(e\gamma)=\dfrac{\varepsilon_m}{2}[\pm C_{m+n}(e)\sin(m+n)\gamma+(-1)^nC_{m-n}(e)\sin(m-n)\gamma]\end{cases}$$

where * represents Layer-S or Layer-V, and $R(1,2)C_{ml,r}^{\pm}(*)$ is $R(1,2)J_{ml,r}^{\pm}(*)$ when $T_{1,*}^{\sim(**)}$ is $T_{1,*}^{\sim(1)}$, and $R(1,2)C_{ml,r}^{\pm}(*)$ is $R(1,2)H_{ml,r}^{(1)\pm}(*)$ when $T_{1,*}^{\sim(**)}$ is $T_{1,*}^{\sim(3)}$. D_{13} , D_{14} are the distance between O_1 and O_3 , O_4, and γ_{13}, γ_{14} are the angle between coordinate system $r_1-\theta_1$ and coordinate systems $r_3-\theta_3$, $r_4-\theta_4$, respectively.

APPENDIX-D. The elements of coefficient matrix

$$\begin{cases} E_{11}^{v_o^{(1)}}(n.r) = \left(n^2 + n - \dfrac{k_\alpha^2 r^2}{2}\right) C_n(k_\alpha r) - k_\alpha r C_{n-1}(k_\beta r) \\ E_{12}^{v_o^{(1)}\mp}(n.r) = \mp n[-(n+1)C_n(k_\beta r) + k_\beta r C_{n-1}(k_\beta r)] \\ E_{21}^{v_o^{(1)}\mp}(n.r) = \mp n[-(n+1)C_n(k_\alpha r) + k_\alpha r C_{n-1}(k_\alpha r)] \\ E_{22}^{v_o^{(1)}}(n.r) = -\left(n^2 + n - \dfrac{k_\beta^2 r^2}{2}\right) C_n(k_\beta r) + k_\beta r C_{n-1}(k_\beta r) \end{cases} \tag{D1}$$

$$\begin{cases} I_{11}^{(i)}(n.r) = -nC_n(k_\alpha r) + k_\alpha r C_{n-1}(k_\alpha r) \\ I_{12}^{(i)\mp}(n.r) = \mp nC_n(k_\beta r) \\ I_{21}^{(i)\mp}(n.r) = \mp nC_n(k_\alpha r) \\ I_{22}^{(i)}(n.r) = -nC_n(k_\beta r) - k_\beta r C_{n-1}(k_\beta r) \end{cases} \tag{D2}$$

Where $C_n(x)$ is $J_n(x)$ when $i = 1$, and $H_n^{(1)}(x)$ when $i = 3$; the superscript v_o indicates the Layer-V at the open region, and correspondingly k_α and k_β indicate $k_{v\alpha} = \omega/\alpha_v$ and $k_{v\beta} = \omega/\beta_v$, respectively, and the others follow the same rule.

References

[1] Bi KM, Hao H. Influence of irregular topography and random soil properties on coherency loss of spatial seismic ground motions. Earthq Eng Struct Dynam 2011; 40(9):1045–61.
[2] Bi KM, Hao H. Modelling and simulation of spatially varying earthquake ground motions at sites with varying conditions. Probabilist Eng Mech 2012;29:92–104.
[3] Liu GH, Lian JJ, Liang C, Zhao M. An effective approach for simulating multi-support earthquake underground motions. Bull Earthq Eng 2017;15(11):4635–59.
[4] Lou L, Zerva A. Effects of spatially variable ground motions on the seismic response of s skewed, multi-span, RC highway bridge. Soil Dynam Earthq Eng 2005;25(7): 729–40.
[5] Yu HT, Yan X, Bobet A, Yuan Y, Xu GP, Su QK. Multi-point shaking table test of a long tunnel subjected to non-uniform seismic loadings. Bull Earthq Eng 2018;16 (2):1041–59.
[6] Yu HT, Yuan Y, Xu GP, Su QK, Yan X, Li C. Multi-point shaking table test for long tunnels subjected to non-uniform seismic loadings-Part II: application to the HZM immersed tunnel. Soil Dynam Earthq Eng 2018;108:187–95.
[7] Boore DM. A note on the effect of simple topography on seismic SH waves. Bull Seismol Soc Am 1972;62:275–84.
[8] Smith WD. The application of finite element analysis to body wave propagation problems. J Roy Astron Soc 1975;42:747–68.
[9] Bouchon M. Effect of topography on surface motion. Bull Seismol Soc Am 1973;63: 615–32.
[10] Géli L, Bard PY, Jullien B. The effect of topography on earthquake ground motion: a review and new results. Bull Seismol Soc Am 1988;78:42–63.
[11] Wong HL, Jennings JC. Effects of canyon topography on strong around motion. Bull Seismol Soc Am 1975;65:1239–57.
[12] Sills LB. Scattering of horizontally-polarized shear waves by surface irregularities. Geophys J Roy Astron Soc 1978;54:319–48.
[13] Boore DM, Larner KH, Aki K. Comparison of two independent methods for the solution of wave-scattering problems: response of a sedimentary basin to vertically incident SH waves. J Geophys Res 1971;76:558–69.
[14] Harsmen SC, Harding ST. Surface motion over sedimentary valley for incident plane P and SV waves. Bull Seismol Soc Am 1981;71:655–70.
[15] Sánchez-Sesma FJ, Ramos-Martínez J, Campillo M. An indirect boundary element method applied to simulated the seismic response of alluvial valleys for incident P, S and Rayleigh waves. Earthq Eng Struct Dynam 1993;22:279–95.
[16] Sánchez-Sesma FJ, Luzón F. Seismic response of three-dimensional alluvial valleys for incident P, SV and Rayleigh waves. Bull Seismol Soc Am 1995;85:269–84.
[17] Bakir BS, Özkan MY, Ciliz S. Effects of basin edge on the distribution of damage in 1995 Dinar Turkey earthquake. Soil Dynam Earthq Eng 2002;22:335–45.
[18] Clayton R, Engquist B. Absorbing boundary conditions for acoustic and elastic wave equations. Bull Seismol Soc Am 1977;67:1529–40.
[19] Virieux J. P-SV wave propagation in heterogeneous media: velocity-stress finite-difference method. Geophysics 1986;51:889–901.
[20] Fellinger JP, Marklein R, Langenberg KJ, Klaholz S. Numerical modeling of elastic wave propagation and scattering with EFIT-elasto dynamic finite integration technique. Wave Motion 1995;21:47–66.
[21] O'Brien GS, Bean CJ. A 3D discrete numerical elastic lattice method for seismic wave propagation in heterogeneous media with topography. Geophys Res Lett 2004;31(14):101–11.
[22] Trifunac MD. Scattering of plane SH waves by a semi-cylindrical canyon. Earthq Eng Struct Dynam 1973;1:267–81.
[23] Wong HL, Trifunac MD. Scattering of plane SH waves by a semi-elliptical canyon. Earthq Eng Struct Dynam 1974;3:157–69.
[24] Tsaur DH, Chang KH. An analytical approach for the scattering of SH waves by a symmetrical V-shaped canyon: shallow case. Geophys J Int 2008;174:255–64.
[25] Tsaur DH, Chang KH, Hus MS. An analytical approach for the scattering of SH waves by a symmetrical V-shaped canyon: deep case. Geophys J Int 2010;183: 1501–11.
[26] Zhang N, Gao Y, Li D, Wu Y, Zhang F. Scattering of SH waves induced by a symmetrical V-shaped canyon: a unified analytical solution. Earthq Eng Eng Vib 2012;11:445–60.
[27] Zhang N, Gao Y, Cai D, Wu Y, Li D. Scattering of SH waves induced by a non-symmetrical V-shaped canyon: a unified analytical solution. Geophys J Int 2012; 191:243–56.
[28] Tsaur DH, Chang KH. Scattering of SH waves by truncated semicircular canyon. J Eng Mech 2009;135:862–70.
[29] Gao Y, Li D, Zhang N, Liu H, Cai Y, Wu Y. Effects of topographic amplification induced by a U-shaped canyon on seismic waves. Bull Seismol Soc Am 2012;102: 1748–63.
[30] Cao H, Lee VW. Scattering of plane SH waves by circular cylindrical canyons with variable depth-to-width ratio. Eur J Earthq Eng 1989;2:29–37.
[31] Cao H, Lee VW. Scattering and diffraction of plane P waves by circular cylindrical canyons with variable depth-to-width ratio. Soil Dynam Earthq Eng 1990;9: 141–50.
[32] Yuan X, Liao Z. Scattering of plane SH waves by a cylindrical canyon of circular-arc cross-section. Int J Soil Dyn 1994;13:407–12.
[33] Pao YH, Mow CC. Diffraction of elastic waves and dynamic stress concentrations. New York Crane Russak and company; 1973. p. 389–95.
[34] Li WH, Zhao CG. Scattering of plane SV waves by cylindrical canyons in saturated porous medium. Int J Soil Dyn 2005;25:981–95.
[35] Liang JW, Zhang YS, Gu XL, Lee VW. Scattering of plane SH waves by a circular-arc layered canyon. J Vib Eng 2003;16(2):158–65.
[36] Liang JW, Yan LL, Lee VW. Scattering of plane P waves around circular-arc layered alluvial valleys: analytical solution. Acta Seismol Sin (Chin Ed) 2001;14:176–95.
[37] Liang JW, Yan LL, Lee VW. Diffraction of plane SV waves by a circular-arc layered alluvial valley: analytical solution. Acta Mech Solid Sin 2003;24:235–43.
[38] Zhang YS. Scattering of plane P waves by canyons containing multiple circular-arc-shaped layers. Earthq Sci 2010;23:157–65.
[39] Vincent WL, Liu WY. Two-dimensional scattering and diffraction of P-and SV-waves around a semi-circular canyon in an elastic half-space: an analytic solution via a stress-free wave function. Soil Dynam Earthq Eng 2014;63:110–9.
[40] Wan YG. Introduction to seismology. Beijing: Science press; 2016.